Advected fields in maps: I. Magnetic flux growth in the stretch–fold–shear map

Andrew D. Gilbert

School of Mathematical Sciences, University of Exeter, EX4 4QE, U.K.

Abstract

The behaviour of magnetic field in the stretch–fold–shear (SFS) dynamo map is considered for zero magnetic diffusion. It is shown by a mixture of analytical and numerical approaches that the SFS map is a perfect dynamo: for sufficiently large shear, the adjoint operator has smooth, growing eigenfunctions and so smooth flux averages grow exponentially with time for zero diffusion.

In the paper first a number of numerical discretisations are presented that give differing results for growth rates, and indicate the need to develop systematic theory. Then magnetic fields that are only required to be square integrable are considered, and the spectral properties of the SFS dynamo operator and its adjoint are discussed, as operators in L^2. Adjoint eigenfunctions are typically not smooth, however. To obtain smooth, growing adjoint eigenfunctions attention is restricted to a subset of magnetic fields that are analytic in a disc in the complex plane. Restricted to this subset and using a supremum norm, the SFS adjoint operator is compact and this allows a numerical treatment of eigenvalues and eigenfunctions with systematic error estimates. These estimates show that for sufficiently large shear there are smooth growing adjoint eigenfunctions and so perfect dynamo action is established.

Key words: Magnetic field, dynamo, hyperbolic map, mixing, baker's map.

1 Introduction

In dynamo theory we are interested in the growth of magnetic fields when they are transported by a fluid flow, as described by the induction equation

$$\partial_t \boldsymbol{B} = \nabla \times (\boldsymbol{u} \times \boldsymbol{B}) + \varepsilon \nabla^2 \boldsymbol{B}, \tag{1.1}$$

where $\boldsymbol{B}$ is the magnetic field, $\boldsymbol{u}$ is the fluid flow, and the diffusivity ε is the inverse of a dimensionless parameter, the magnetic Reynolds number (e.g., [27]). We shall be concerned only with kinematic theory, in which the fluid

flow $\boldsymbol{u}$ is prescribed. At long times the exponential growth rate of magnetic energy will be $2\gamma(\varepsilon)$ starting from a general initial condition; $\gamma(\varepsilon)$ is the (real) dynamo growth rate.

In the case of an ideal fluid $\varepsilon = 0$, and the induction equation merely represents frozen transport of the magnetic field in the flow. Starting from a general initial condition the field becomes ever finer scaled and increasingly complicated. If the flow $\boldsymbol{u}$ is of any complexity, for example being chaotic, or steady with hyperbolic stagnation points, then the magnetic energy increases exponentially when there is zero diffusion, $\gamma(0) > 0$ [35]. If weak diffusion $0 < \varepsilon \ll 1$ is now introduced, because of the process of fine-scaling, its effects can be very subtle. For example it is known that if the flow takes too simple a form, for example lying wholly in parallel planes, then any finite diffusion causes the field ultimately to decay, with $\gamma(\varepsilon) < 0$ for any $\varepsilon > 0$, no matter how complex the flow in each parallel plane [13,36]. This highlights the fact that $\gamma(\varepsilon)$ is generally discontinuous at $\varepsilon = 0$. The singular nature of the limit $\varepsilon \to 0$ is of course also suggested by the form of the induction equation (1.1) above.

The existence of kinematic dynamos, flows $\boldsymbol{u}$ which amplify magnetic fields for some ε and initial condition, is now not in doubt, but there are many open questions about their behaviour in the astrophysically important limit $\varepsilon \to 0$. Of particular interest are 'fast dynamos' in which the growth rate $\gamma(\varepsilon)$ of magnetic energy remains positive and of order unity in this limit (see e.g., [12,37]). Such dynamos rely on the flow $\boldsymbol{u}$ to stretch and fold magnetic field in such a way that field growth is robust to the effects of weak diffusion. It is known that for a fast dynamo in a smooth flow $\boldsymbol{u}$, it is necessary that the flow have positive topological entropy, and this gives an upper bound on the limiting growth rate as $\varepsilon \to 0$. This was conjectured by Finn & Ott [14], and proved by Klapper & Young [23]. Very little otherwise is known analytically about the existence of fast dynamos in smooth flows, although Dr. Oleg Kozlovsky (personal communication) has recently proved results about a three-dimensional flow with a 'pretzel' structure.

On the other hand there is good computational evidence for fast dynamos in a number of smooth flows, in particular taking the convenient form $\boldsymbol{u}(x, y, t) = (u_x, u_y, u_z)$, that is flows that are two-dimensional, depending on two coordinates, but not confined to a plane [16,30]. Study of these and similar flows suggests that field amplification is through the 'stretch–fold–shear' mechanism [7,8,15]. The idea is that field lines in the plane become stretched and folded through the u_x and u_y components of the flow (for example through tendrils of field formed at a broken heteroclinic connection). This planar flow alone could not give dynamo action [13,36], as it creates bands of field of opposing sign which are vulnerable to diffusive cancellation. The second process which acts to reduce cancellations is a shear of the field in the z-direction, through the u_z flow component. If the magnetic field depends on z then motion in z

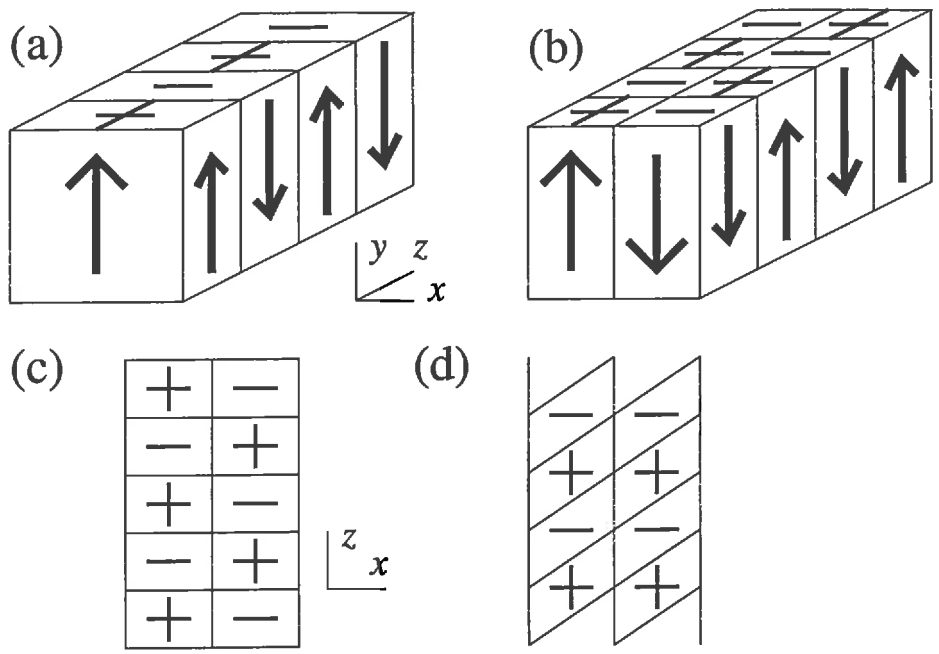

Fig. 1. The stretch–fold–shear map. (a) Magnetic field depending on z is stretched and folded with a baker's map in the (x, y)-plane to give (b). In (c) the field orientation is shown in the (x, z)-plane, which after the shear operation gives (d). The effect of the stretch–fold–shear operations from (a) to (d) is to double the magnitude of field vectors and partially bring like-signed field together.

can now bring like-signed field together.

This constitutes the stretch–fold–shear (SFS) mechanism, and to illustrate and study it further Bayly & Childress [7] introduce a simplified version known as the stretch–fold–shear (SFS) map. This is illustrated in figure 1, and we shall define it in section 2 below. In going from a smooth flow $\boldsymbol{u}$ to a map, we note that magnetic field is moved in the obvious way, using the tangent map, and that diffusion may be employed by integrating the field against a heat kernel between mappings. This model is much simplified compared to a general flow $\boldsymbol{u}$, because the chaotic stretching is now based on a hyperbolic, baker's map. However it is still difficult to deal with analytically because of the complicated oscillations that arise in the magnetic field after only a few iterations. Diffusion will have a strong effect because of the rapid variation in the magnetic field, but there may also be additional effects because the SFS map is discontinuous.

In this paper, which we label I, and a companion paper II [18] our aim is to establish results about the behaviour of magnetic fields in the SFS model depicted in figure 1. A third, paper [19] will consider the evolution of passive scalars. In order to navigate our way through papers I and II, it is worth at this point giving a few precise definitions.

We have in mind applying a map M. Under this map a magnetic field b evolves under the operator T_ε for diffusivity $\varepsilon \geq 0$. After n time units the magnetic field is $T_\varepsilon^n b$ and we may define the dynamo growth rate by

$$\gamma(\varepsilon) = \sup_b \limsup_{n\to\infty} n^{-1} \log \|T_\varepsilon^n b\|. \tag{1.2}$$

Here we are using an L^2 norm in the space under consideration

$$\|b\|^2 = (b,b), \qquad (f,g) = \int \overline{f(x)} g(x)\, dx, \tag{1.3}$$

to measure magnetic energy and the supremum above may be taken over all initial conditions having finite energy. The map is a *dynamo* if $\gamma(\varepsilon) > 0$ for some $\varepsilon > 0$.

If we take the ideal limit $\varepsilon \to 0$ we may define the *fast dynamo growth rate* by

$$\gamma_0 = \liminf_{\varepsilon\to 0} \gamma(\varepsilon) \tag{1.4}$$

which is generally not equal to $\gamma(0)$, as discussed above. The map is a *fast dynamo* if $\gamma_0 > 0$. One problem is to show that a given map M is a fast dynamo. Another problem is to relate the exponent γ_0 to properties of the map M and the evolution of magnetic field with zero diffusion $\varepsilon = 0$. This involves quantifying the rapid fluctuation in sign of field in $T_0^n b$ for large n. Since averaging is superficially similar to diffusion [6,8,14] one may study the *perfect dynamo growth rate*

$$\Gamma = \sup_c \sup_b \limsup_{n\to\infty} n^{-1} \log |(c, T_0^n b)|, \tag{1.5}$$

that is, consider the growth rate of a fixed average or projection of the magnetic field as it evolves. We then take the supremum over initial conditions and projections that are smooth functions $b, c \in C^\infty$ [8]. If $\Gamma > 0$ then we say that the map is a *perfect dynamo* and exhibits *flux growth.*

One may then make conjectures about the relation of Γ and γ_0: the strongest would be that the two growth rates are equal under certain circumstances (see [6,8,10,12,14]). We shall discuss these more fully in the introduction to paper II. Before leaving this section we note that the supremum over smooth functions in (1.5) above is not the only possibility. In [14] it is argued that the growth rates of flux through general surfaces should be measured, and there is numerical evidence that with this definition $\Gamma = \gamma_0$ in a number of physically reasonable flows (chapter 2 of [12]). This would correspond to allowing c in the above definition to be certain distributions. Also one might replace a strict

supremum by a notion of the flux through 'generic' surfaces, in some sense [14]. However at present there is a lack of mathematical results to guide us.

1.2 Structure of the paper

Our aim in this paper and II is to investigate $\gamma(\varepsilon)$, γ_0 and Γ and their relationships for SFS and related dynamo models. The two papers have distinct flavours. We consider first this paper, paper I, which builds on the studies [10,12].

Here we consider only the case of zero diffusion, $\varepsilon = 0$, and we set $T \equiv T_0$ for succintness. Our principal aim is to show that the SFS model is a perfect dynamo. We note that since $(c, Tb) = (T^*c, b)$ where T^* is the adjoint operator in L^2, instead of investigating $T^n b$ in (1.5) we may equally well consider $T^{*n}c$. The adjoint operator T^* tends to smooth out small-scale structure, unlike the direct operator T, and so is much easier to handle [8]. In this paper, using a mixture of analytical and numerical methods, we exhibit smooth growing eigenfunctions of the adjoint operator T^* for large enough shear and so establish perfect dynamo action.

The paper is structured as follows. In section 2 we define the SFS map M and the operators T and T^*. The operator T^* may be discretised in a number of plausible ways, but these give rather differing numerical results for eigenvalues (see section 3). This highlights the need for a firm theoretical basis for any numerical method adopted. In section 4 we summarise basic results about SFS and give some exact solutions. We then study T and T^* as operators in L^2 and their spectra in section 5. In view of the definition of a perfect dynamo above we are particularly interested in how smooth are any eigenfunctions that may exist. We find that the operators have a large spectrum, in particular T^* has a whole disc of point spectrum. However when we attempt to construct eigenfunctions explicitly, we find that generally they are not smooth and so do not provide information about the perfect dynamo growth rate Γ defined above.

To establish that $\Gamma > 0$ and so that SFS is a perfect dynamo, we need to obtain smooth eigenfunctions of T or T^*, but these are like needles in the L^2 haystack. We therefore restrict our attention to a subset of L^2, namely functions that are not only smooth, but in addition are analytic in a disc on the complex plane, and we use a supremum norm (section 6). We denote T^* restricted to this space by S, and seek eigenfunctions of S. This gives an operator with the useful property of compactness and this allows us to focus on its point spectrum, simply eigenvalues and eigenfunctions. This important simplification has been exploited elsewhere in dynamical systems theory (e.g.,

[26,29]).

We may then study a discrete approximation S_N to S, and use perturbation theory (section 7) to bound errors in these approximations. We thus obtain smooth growing eigenfunctions of S and so of T^*, which allows to establish flux growth or perfect dynamo action in the SFS model by virtue of definition (1.5). In section 8 we discuss subsidiary issues, including growth rates for large shears and nonlinear shears. Section 9 gives concluding discussion.

Whereas in this paper the emphasis is on $\varepsilon = 0$, in paper II we introduce diffusion $\varepsilon > 0$; our aim is to compute $\gamma(\varepsilon)$ and the fast dynamo growth rate γ_0 for varying boundary conditions, and to understand how γ_0 relates to Γ. Does perfect dynamo action $\Gamma > 0$ imply fast dynamo action $\gamma_0 > 0$? Are the two growth rates generally equal? Can we take a smooth eigenfunction of T^* for $\varepsilon = 0$ and use perturbation theory to obtain an approximate eigenfunction of T_ε^* for $0 < \varepsilon \ll 1$? In paper II we will use standard asymptotic approximations, but without rigorous justification. Rather, our aim there is to piece together a picture of how perfect dynamo action and weak diffusion interact, supported by numerical simulations.

Finally we mention that there are some related models for which some rigorous results are known. Childress [11] has shown fast dynamo action in a map similar to SFS but with many folds, while in [17] results are obtained for a model based on a pseudo-Anosov map with shear in the limit of strong stretching. Much is also known about generalised baker's maps [14].

2 The stretch–fold–shear map

2.1 Definition of the SFS map M and operator T

The SFS map M is shown in figure 1. Its domain is given by $(x, y) \in [-1, 1]^2$ and $z \in \mathbb{R}$, and is the composition of two basic operations $M = M_{\mathrm{Sh}} M_{\mathrm{SF}}$. The first is a folded baker's map

$$M_{\mathrm{SF}}(x, y, z) = \begin{cases} (\frac{1}{2}(x-1), 1+2y, z) & (y < 0), \\ (\frac{1}{2}(1-x), 1-2y, z) & (y \geq 0), \end{cases} \tag{2.1}$$

and the second is shear in the z-direction

$$M_{\mathrm{Sh}}(x, y, z) = (x, y, z + \alpha x), \tag{2.2}$$

where α is the shear parameter.

Now magnetic field is mapped, frozen under M. Since M_{SF} doubles the y-components and x-gradients of field and halves the x-components and y-gradients, we need only consider fields of the simplified form

$$\boldsymbol{B}(x,y,z) = e^{ikz}(b(x)\hat{\boldsymbol{y}} + b_3(x)\hat{\boldsymbol{z}}) + \text{complex conjugate}, \tag{2.3}$$

where k is a wavenumber in the z-direction and b and b_3 are complex fields. We may also take $k = 1$ without loss of generality, since only the combination αk arises for $\varepsilon = 0$. The maps M_{SF} and M_{Sh} induce maps of the field component b by the operators

$$T_{\mathrm{SF}}b(x) = \begin{cases} 2b(1+2x) & (x<0), \\ -2b(1-2x) & (x \geq 0), \end{cases} \tag{2.4}$$

$$T_{\mathrm{Sh}}b(x) = e^{-i\alpha x}b(x), \tag{2.5}$$

while the b_3 component need not be considered; it is not stretched and is slaved to the b component (being generated only during the shear process). The magnetic field is transported in (2.4) according to the tent map in x,

$$\tau(x) = \min(1+2x, 1-2x), \tag{2.6}$$

which is the x-component of M_{SF}^{-1} and is continuous at $x = 0$.

We may then define the SFS operator $T \equiv T_0 = T_{\mathrm{Sh}}T_{\mathrm{SF}}$ on magnetic fields. This is the main operator we shall study in this paper and it is given by

$$Tb(x) = \begin{cases} 2e^{-i\alpha x}b(1+2x) & (x<0), \\ -2e^{-i\alpha x}b(1-2x) & (x \geq 0). \end{cases} \tag{2.7}$$

The order of operations is not important, and occasionally it is useful to reverse the order, and set $T = T_{\mathrm{SF}}T_{\mathrm{Sh}}$.

When we employ non-zero diffusion ε in paper II, we will apply a third step, of diffusion for a unit time with appropriate boundary conditions at $x = \pm 1$. This gives the diffusive dynamo operator $T_\varepsilon = H_\varepsilon T$. Note that earlier studies of SFS worked on the interval $[0,1]$ for x and y whereas we will find $[-1,1]$ more convenient. Also our parameter α corresponds to what was $\pi k\alpha$ or $\pi\alpha$ in previous studies [7,8]. We consider only $\alpha \geq 0$ without loss of generality.

2.2 Definition of the adjoint operator T^*

The operator T contracts the scale of variation of magnetic field in the x-direction as T is iterated on some initial condition b. Together with the phase

shifts from the shear in (2.7) this leads to a complicated field $T^n b$ for large n. For perfect dynamo action we are seeking growth in

$$\Phi_n = (c, T^n b) = (T^{*n} c, b) \tag{2.8}$$

for some smooth fields b, c, as n increases. Here $(\cdot, \cdot)$ is the inner product defined back in (1.3) with the integral taken from -1 to 1. If c is chosen so that $(c, 1) = 1$, then $(c, T^n b)$ is a projection of $T^n b$; we will loosely refer to $(c, \cdot)$ as a projection without insisting on this condition. Note that the case $c = 1$ gives the total flux of b through $[-1, 1]$. From (2.8) we can either seek growth in $T^n b$ or in $T^{*n} c$ where T^* is the adjoint operator given by

$$T^* c(x) = e^{i\alpha\frac{1}{2}(x-1)} c(\tfrac{1}{2}(x-1)) - e^{i\alpha\frac{1}{2}(1-x)} c(\tfrac{1}{2}(1-x)). \tag{2.9}$$

This is the composition of two operators $T^* = T^*_{\rm SF} T^*_{\rm Sh}$ with

$$T^*_{\rm SF} c(x) = c(\tfrac{1}{2}(x-1)) - c(\tfrac{1}{2}(1-x)), \quad T^*_{\rm Sh} c(x) = T^{-1}_{\rm Sh} c(x) = e^{i\alpha x} c(x). \tag{2.10}$$

The adjoint operator T^* is attractive for analysis because $T^*_{\rm SF}$ halves gradients in the x direction, unlike $T_{\rm SF}$. One may expect that eigenfunctions exist in which this stretching out of structure is in balance with its introduction through multiplication by $e^{i\alpha x}$ in $T^*_{\rm Sh}$. It is thus expected that T^* should have some smooth eigenfunctions, and this should facilitate analysis [8]. If a smooth eigenfunction exists that grows under iteration of T^*, then we have shown that SFS is a perfect dynamo by the definition (1.5).

There are other models closely related to SFS. We can change the baker's map from a folded baker's map to a stacked baker's map, which we define and discuss briefly in appendix A. This model is less physically realistic and less interesting than SFS, but is used in paper II for comparison with SFS when diffusion is introduced. In a similar vein we note that the shear operation may be generalised, replacing αx by $f(x)$ in (2.2) and so replacing $T_{\rm Sh}$ by

$$T_{\rm Sh} b(x) = e^{-if(x)} b(x). \tag{2.11}$$

We shall comment below on more general shears, and here only note that taking $f(x) = \alpha\ \mathrm{sign}(x)$ gives the stretch–fold–slide map studied in [12,21,22].

3 Computing growth rates

We have argued above that T^* should have some smooth eigenfunctions, and this suggests that it should be easy to obtain robust growth rates numerically. It turns out however that the results depend rather sensitively on the numerical procedure adopted.

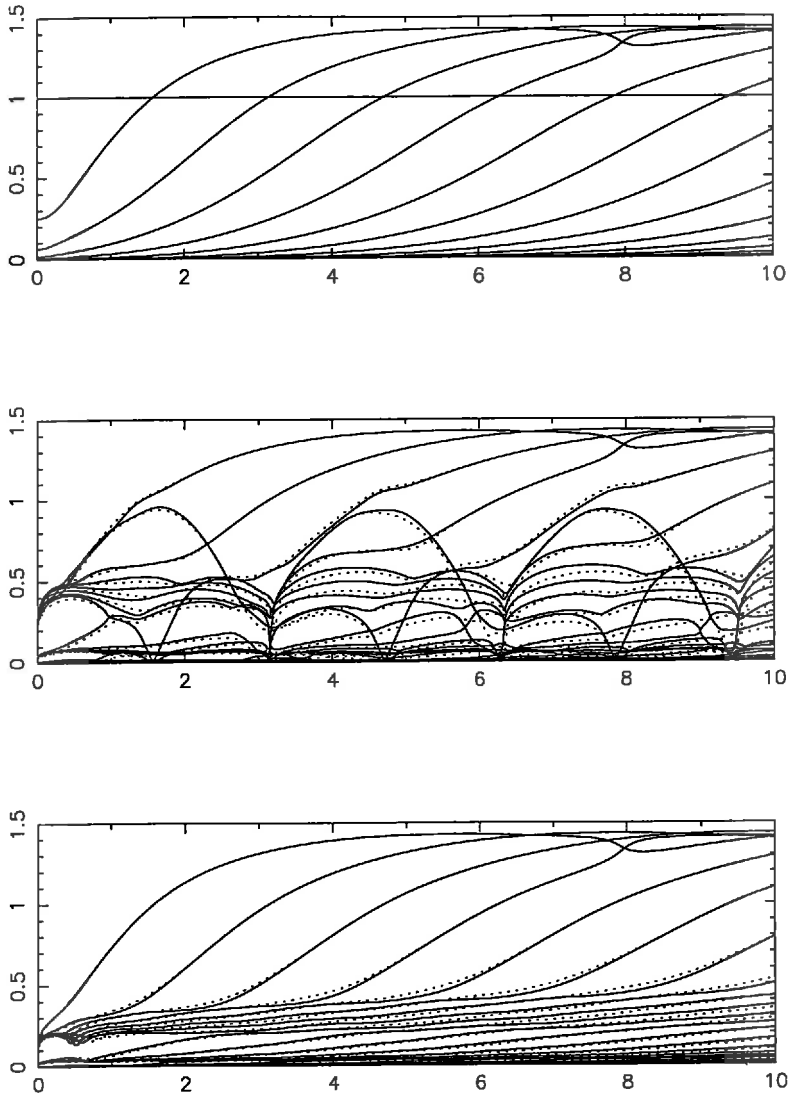

Fig. 2. (a,b,c). Computations of eigenvalues λ using different discretisations of T^*. Absolute values $|\lambda|$ are plotted against α using discretisations with matrices of size 128^2 (solid) and 64^2 (dotted) to give an indication of convergence. The methods used are (a) power series, (b) Fourier series, and (c) sine series. Only the 30 largest values of $|\lambda|$ are shown; the resoution in α is 0.01.

We give a number of possible methods below. In each case we express c as a sum of basis functions with complex coefficients c_n. If $T^*c = d$ then we may compute the matrix elements A_{mn} so that

$$d_m = \sum_{n=0}^{\infty} A_{mn} c_n. \tag{3.1}$$

Truncating the infinite matrix by restricting the ranges of m and n leads to a finite eigenvalue problem that may be tackled numerically to obtain eigenvalues λ and eigenfunctions $c(x)$, which we order in terms of decreasing $|\lambda|$.

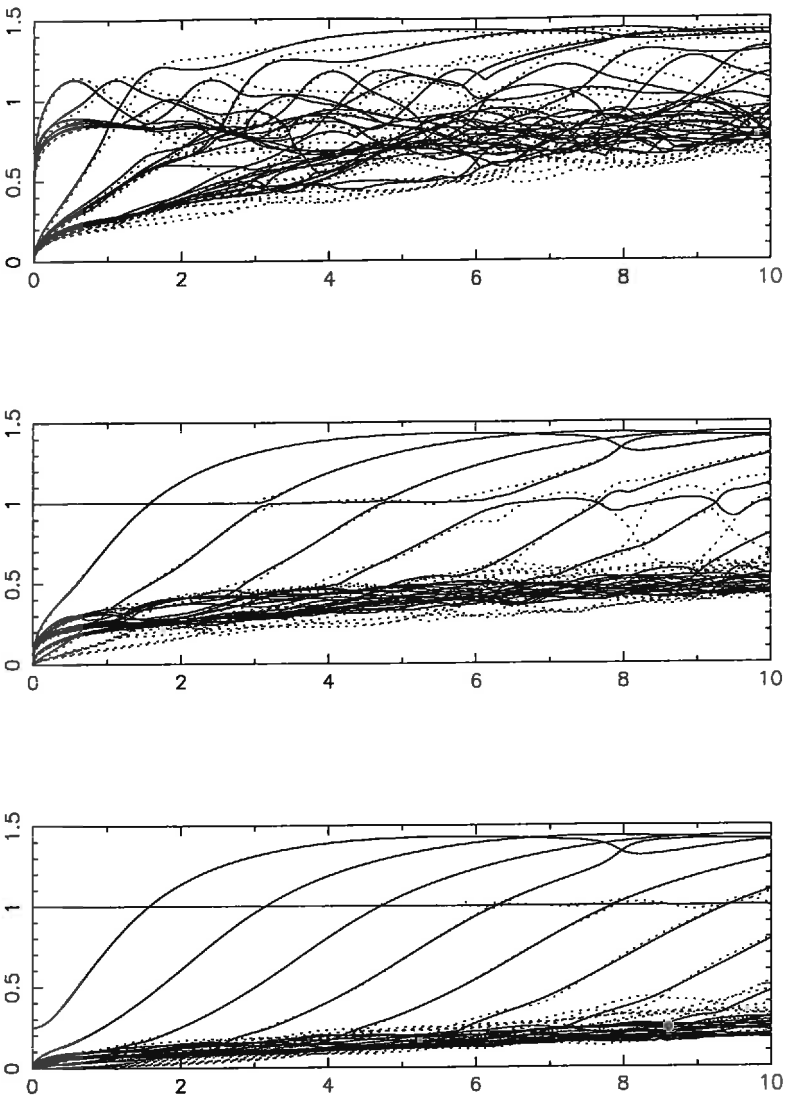

Fig. 3. (a,b,c). Computations of eigenvalues λ using different discretisations of T^*. As in figure 2, but using (a) piecewise constant, (b) piecewise linear, and (c) piecewise cubic.

Figures 2 and 3 show the result of using six different discretisations, listed in the figure captions and detailed below. In each case the solid lines show the results when the matrix A_{mn} is truncated to 128^2 while the dotted lines show a truncation of 64^2. Only the 30 eigenvalues with the largest values of $|\lambda|$ are shown. There is a wide range of results, even though in each individual case the results appear to be converging as the resolution is increased from 64 to 128, although poorly in 3(a). All discretisations except 3(a) also agree when $|\lambda| \gtrsim 1.3$. This is encouraging as an eigenvalue $|\lambda| > 1$ corresponds to perfect dynamo action provided the corresponding eigenfunction is smooth. The results for these larger values of λ agree with those elsewhere in the literature [7,8]. Of the figures 2(a) has the edge on aesthetic grounds and 3(a) certainly is the least pleasant. Figures 3(b) and 3(c) appear to be converging

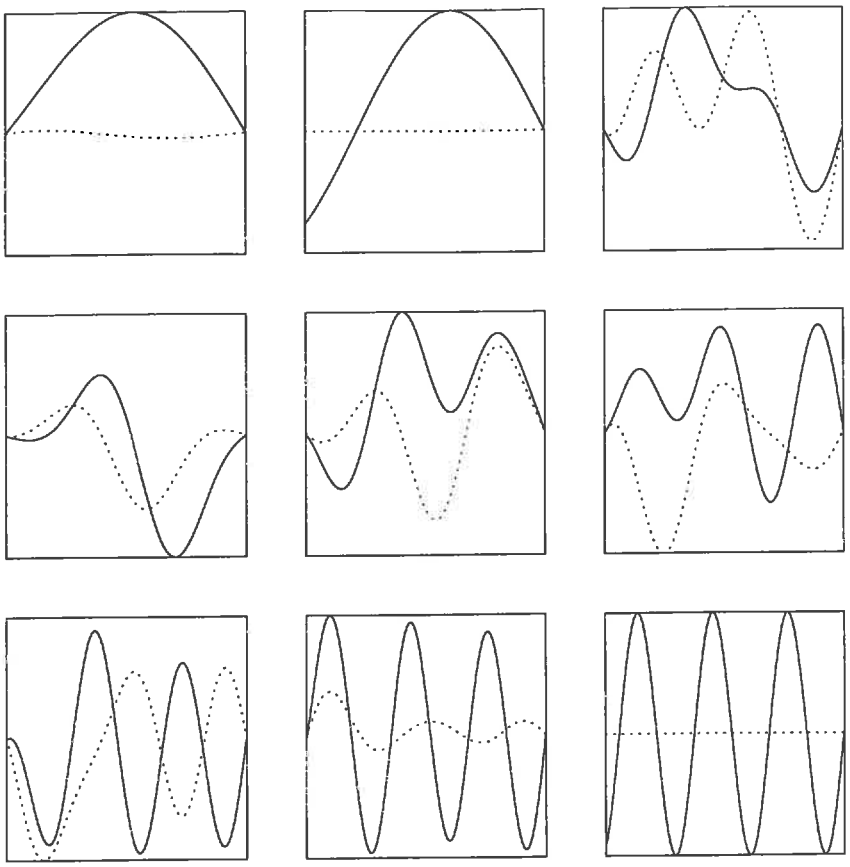

Fig. 4. Eigenfunctions $c_j(x)$ of the SFS adjoint operator plotted against x in the range $-1 \leq x \leq 1$, computed using the power series discretisation. Eigenfunctions with (a) $j = 0$ and (b) $j = 1$ are shown for $\alpha = 2$. In (c–i) $j = 0$ to $j = 6$ are shown for $\alpha = 10$. The real part is shown solid, and the imaginary part dotted. The top row is (a,b,c), middle (d,e,f) and bottom (g,h,i).

to 2(a) except for a belt of 'noise' for small $|\lambda|$. On the other hand 2(a) and 3(b,c) have a straight line $|\lambda| = 1$ which is not seen in 2(b,c) or 3(a).

Clearly we need some theory to determine which figure gives sensible results and this will be developed in sections 6 and 7. It will turn out that the power series discretisation yielding figure 2(a) can be put on a firm basis, and these branches correspond to eigenvalues of T^* with eigenfunctions that are smooth, and indeed entire as functions of a complex variable. The growing eigenfunctions for $\alpha = 2$ and 10 are shown for this discretisation in figure 4. We will also be able to put error bounds on the numerical computations in figure 2(a): we will thus establish the presence of growing smooth eigenfunctions of T^*, and so perfect dynamo action.

The two discretisations based on piecewise linear (e) and piecewise cubic (f) functions are converging to 2(a) as the resolution is increased. We now list briefly the six discretisations used in figures 2 and 3.

3.1 *Figure 2(a): power series approximation.*

Set

$$c(x) = \sum_{n=0}^{\infty} c_n x^n; \tag{3.2}$$

the matrix elements become

$$A_{mn} = \sum_{p=\max(m-n,0)}^{m} \frac{2^{-n}(-1)^m n!}{p!(m-p)!(n-m+p)!} \left(\frac{i\alpha}{2}\right)^p [e^{-i\alpha/2}(-1)^{n+p} - e^{i\alpha/2}]. \tag{3.3}$$

These matrices are truncated and eigenvalues extracted numerically using NAG library routines, shown in figure 2(a). Some eigenfunctions are shown in figure 4.

3.2 *Figure 2(b): Fourier series approximation.*

Put

$$c(x) = \sum_{n=-\infty}^{\infty} c_n e^{in\pi x}; \tag{3.4}$$

then

$$A_{mn} = e^{-i\frac{1}{2}(\alpha+n\pi)} F(\alpha/2 - m\pi + n\pi/2) - e^{i\frac{1}{2}(\alpha+n\pi)} F(-\alpha/2 - m\pi - n\pi/2), \tag{3.5}$$

with

$$F(s) = s^{-1} \sin s. \tag{3.6}$$

3.3 *Figure 2(c): sine series approximation.*

In this approximation we temporarily exchange stretch–fold and shear operations to define $T^* = T^*_{\mathrm{Sh}} T^*_{\mathrm{SF}}$. This operator annihilates even functions. In seeking eigenvalues $\lambda \neq 0$ we may project to odd functions and, using obvious notation, find eigenvalues of $P_{\mathrm{odd}} T^*$ (since if $P_{\mathrm{odd}} T^* c_{\mathrm{odd}} = \lambda c_{\mathrm{odd}}$ and $\lambda \neq 0$ then $c = c_{\mathrm{odd}} + c_{\mathrm{even}}$ is an eigenfunction of T^* where $c_{\mathrm{even}} = \lambda^{-1} P_{\mathrm{even}} T^* c_{\mathrm{odd}}$ (p. 266 of [12]).

We then represent c by a sine series

$$c(x) = \sum_{n=1}^{\infty} c_n \sin(n\pi x), \tag{3.7}$$

for which

$$\begin{aligned} A_{mn} = &-e^{-in\pi/2}F(\alpha + m\pi + n\pi/2) + e^{-in\pi/2}F(\alpha - m\pi + n\pi/2) \\ &+e^{in\pi/2}F(\alpha + m\pi - n\pi/2) - e^{in\pi/2}F(\alpha - m\pi - n\pi/2). \end{aligned} \tag{3.8}$$

3.4 Figure 3(a,b,c): spatial discretisations.

The above discretisations in figure 2(a,b,c) involve a series expansion of a global nature for the function $c(x)$. An alternative is to employ an expansion allowing more local freedom by dividing $[-1,1]$ into a set of subintervals, and letting the function $c(x)$ on each interval to be, for example, in figure 3(a) constant, (b) linear or (c) cubic. Here we set up a framework for such approximations. We return to consider the operator T acting on a magnetic field. Let M be an integer divisible by 4 and $\delta = 1/M$. We break the interval $[-1,1]$ into M intervals I_j indexed by j with $-M/2 \le j \le M/2 - 1$. The jth strip is given by $I_j = [2j\delta, 2(j+1)\delta]$ and has midpoint $(2j+1)\delta$. We will let $b_j(x)$ give the field in strip j, but rescaled so that x runs over $[-1,1]$, specifically

$$b_j(x) = b((2j+1+x)\delta) \qquad (x \in [-1,1]), \tag{3.9}$$

and conversely

$$b(x) = b_j(x/\delta - 2j - 1) \qquad (x \in I_j). \tag{3.10}$$

We refer to this set of functions $\tilde{b} = \{b_j\}$ as a *magnetic field discretisation.*

The basic operators T_{SF} and T_{Sh} become

$$\tilde{T}_{\mathrm{SF}} b_j(x) = \begin{cases} 2b_{M/2+2j}(1+2x) & (j<0, x<0), \\ 2b_{M/2+2j+1}(-1+2x) & (j<0, x>0), \\ -2b_{M/2-2j-1}(-1-2x) & (j\ge 0, x<0), \\ -2b_{M/2-2j-2}(1-2x) & (j\ge 0, x>0), \end{cases} \tag{3.11}$$

$$\tilde{T}_{\mathrm{Sh}} b_j(x) = e^{-i\alpha\delta(2j+1+x)} b_j(x) \tag{3.12}$$

and may be combined to give $\tilde{T}$.

We define an adjoint set of functions $\tilde{c} = \{c_j\}$, discretised from $c(x)$ as above,

and the corresponding inner product is

$$(\tilde{c}, \tilde{b}) = \sum_j \delta \int_{-1}^{1} \overline{c_j(x)} b_j(x)\, dx. \tag{3.13}$$

In terms of these functions

$$\tilde{T}^*_{\rm SF} c_j(x) = \begin{cases} c_{\frac{1}{4}(-M+2j)}(\frac{1}{2}(x-1)) - c_{\frac{1}{4}(M-2j-4)}(\frac{1}{2}(-x+1)) & (j \text{ even}), \\ c_{\frac{1}{4}(-M+2j-2)}(\frac{1}{2}(x+1)) - c_{\frac{1}{4}(M-2j-2)}(\frac{1}{2}(-x-1)) & (j \text{ odd}), \end{cases} \tag{3.14}$$

while $\tilde{T}^*_{\rm Sh} = \tilde{T}^{-1}_{\rm Sh}$.

We will spare the reader the details, but the idea is now to expand each function c_j as a power series with N terms on the interval $[-1, 1]$. We apply $T^* = T^*_{\rm SF} T^*_{\rm Sh}$ and truncate the each of the resulting set of functions as power series with N terms. This gives a matrix of size $(MN)^2$ with a block structure. Each block has entries similar to those in (3.3) above (but with sign differences), while the indices in (3.14) shuffle the blocks. The results for $N = 1$, 2 and 4 are shown in figure 3(a,b,c) respectively for $MN = 128$ (solid) and 64 (dashed).

4 Elementary properties of T^*

In this short section we consider 'well-behaved' eigenfunctions of T^*, point out some elementary properties and give some exact solutions. Often explicit calculations are possible when $\alpha = 0$, there is no shear in the problem and we have only the stretch–fold operation, with $T = T_{\rm SF}$ (2.4) and $T^* = T^*_{\rm SF}$ (2.10). However this case is of limited interest since perfect dynamo action is impossible (see section 4.3) and with diffusion all fields decay (see paper II).

4.1 Exact eigenfunctions

First note that if $c(x)$ is an eigenfunction of T^*, $T^* c = \lambda c$, then directly from (2.9) we obtain [12,28]

$$c(1) = 0 \qquad (\lambda \neq 0), \tag{4.1}$$

$$c(-1) = 0 \qquad (\lambda \neq 0, e^{-i\alpha}). \tag{4.2}$$

This is confirmed by the numerical eigenfunctions plotted in figure 4; all satisfy (4.1). They all satisfy (4.2), except for figure 4(b,i), which have $\lambda = e^{-i\alpha}$. We

know this since there is an exact solution to $T^*c = \lambda c$ with

$$c(x) = e^{i\alpha(x-1)} - e^{i\alpha(1-x)} = 2i \sin \alpha(x-1), \quad \lambda = e^{-i\alpha} \tag{4.3}$$

(noted by B.J. Bayly, personal communication, and [28]). This solution branch with $|\lambda| = 1$ is only picked up by the power series and spatial discretisations in figure 2(a) and 3(b,c), confirming that the other discretisations are at the very best, incomplete. This eigenfunction is intriguing as it is of marginal stability $|\lambda| = 1$. It appears that there may be a similar mode present for other more general phase shifts; see section 8.2.

This eigenfunction (4.3) satisfies (4.1). Condition (4.2) is not applicable, but happens to be satisfied when $\alpha = n\pi/2$ and this is where branch crossings appear to occur in figure 2(a). We do not have an analytical description of the mode crossings (for an approximate theory, see [28]). However our numerical study of eigenfunctions (for the power series approximation) indicates that the two eigenvalues become coincident (in the complex plane) when $\alpha = n\pi/2$ and so do the corresponding eigenfunctions. This suggests that the operator has a Jordan normal form block $\left(\begin{smallmatrix} \lambda & 0 \\ 1 & \lambda \end{smallmatrix}\right)$ in the $\lambda = e^{-i\alpha}$ eigenspace at this point. Note that the coincidence of two eigenvalues of a general complex matrix is an event of co-dimension two, whereas we are varying a single parameter α. Thus these repeated mode crossings at $\alpha = n\pi/2$ probably have some mathematical significance that we have not elucidated.

Equation (4.3) gives the only smooth eigenfunction we know analytically for general α. However for $\alpha = 0$ there are eigenfunctions taking a polynomial form

$$c_0(x) = x - 1, \quad \lambda = 1, \tag{4.4a}$$
$$c_1(x) = x^3 - 3x^2 - x + 3, \quad \lambda = \tfrac{1}{4}, \tag{4.4b}$$
$$c_2(x) = x^5 - 5x^4 - \tfrac{10}{3}x^3 + 30x^2 + \tfrac{7}{3}x - 25, \quad \lambda = \tfrac{1}{16}. \tag{4.4c}$$

The first of these is also the limit of (4.3) as $\alpha \to 0$. These are most easily obtained by noting that for $\alpha = 0$ if $Tc = \lambda c$ then $Tc'' = 4\lambda c''$, so the eigenfunction $c_n(x)$ may be obtained by integrating $c_{n-1}(x)$ twice and applying the two conditions (4.1, 4.2).

4.2 Discontinuous eigenfunctions of T^*

It is also possible to construct discontinuous eigenfunctions of T^*. First consider an eigenfunction with a finite number q of discontinuities at points $x_1, x_2, \ldots, x_q$ in the interior of $[-1, 1]$. Plainly these points must be permuted under the tent map τ (2.6) (otherwise their number would reduce under T^*) and so must constitute a union of periodic orbits of τ. Arguing similarly, in

(2.9) the discontinuity at x_n in T^*c must come from just one of the two terms on the right-hand side, not both. Thus, using $[\cdot]_{x_n}$ to denote the jump in a quantity across a discontinuity, we have

$$[T^*c(x)]_{x_n} = \lambda[c(x)]_{x_n} = e^{\frac{i\alpha}{2}(x_n-1)}[c(\tfrac{1}{2}(x-1))]_{x_n} \text{ or } e^{\frac{i\alpha}{2}(1-x_n)}[c(\tfrac{1}{2}(1-x))]_{x_n}. \tag{4.5}$$

Hence the absolute value of the jump is a constant around a periodic orbit and it is clear that any such eigenfunction must have $|\lambda| = 1$.

As an example, if $q = 1$, the discontinuity must lie at the fixed point $x_1 = 1/3$ and so we obtain $\lambda = e^{i\alpha/3}$. If $q = 2$ the discontinuities must lie on the period-2 orbit $\{-\frac{1}{5}, \frac{3}{5}\}$ and $\lambda^2 = e^{2i\alpha/5}$. One may give a similar discussion if the discontinuity occurs only in a derivative; if the eigenfunction is C^{r-1} but has finitely many discontinuities in its rth derivative $c^{(r)}$ then $|\lambda| = 2^{-r}$. The above describes such eigenfunctions, if they exist. Examples may be constructed for $\alpha = 0$, for example,

$$c(x) = \begin{cases} 1 & x < 1/3, \\ 0 & x > 1/3, \end{cases} \qquad \lambda = 1, \tag{4.6}$$

$$c(x) = \begin{cases} 1 + x & x < 1/3, \\ 2 - 2x & x > 1/3, \end{cases} \qquad \lambda = -\tfrac{1}{2}. \tag{4.7}$$

Numerically it appears that solution branches extend out from $\alpha = 0$ to give discontinuous eigenfunctions for any α; see figure 8 in section 8.3 below.

4.3 Decay for $\alpha = 0$

In this section we show that SFS is not a perfect dynamo for $\alpha = 0$ [12]. A proof of this obvious result is worthwhile as this is a test case for theory below, especially as we shall obtain growing eigenfunctions of T^* for $\alpha = 0$ in L^2 below! Here we show that for any smooth b and c, $(c, T^n b)$ is bounded and so the perfect dynamo growth rate Γ defined in (1.5) cannot be positive. We define a potential a for b by

$$a(x) = \int_{-1}^{x} b(x)\, dx. \tag{4.8}$$

When T is applied to b, the potential is mapped as a passive scalar, by

$$T_{\text{scalar}} a(x) = a(\tau(x)), \tag{4.9}$$

where the tent map τ is defined in (2.6).

Consider a sequence of iterates $b_n = T^n b$ with corresponding potentials $a_n = T^n_{\text{scalar}} a$. Plainly the functions a_n are all bounded by the range of the initial condition a. Hence

$$(c, T^n b) \equiv (T^{*n} c, b) = (c, b_n) = (c, a_n') = -(c', a_n) + [\overline{c(x)} a_n(x)]^1_{-1} \qquad (4.10)$$

(using integration by parts) and the right-hand side is plainly bounded, independent of n, as required. Note that this argument only needs c to be C^1, not smooth.

Also, if we use a piecewise constant function c to measure the flux through a given interval $J = [x_0, x_1] \subset [-1, 1]$, with $c = 1$ inside J and zero outside, then we have

$$(c, T^n b) = (c, a_n') = a_n(x_1) - a_n(x_0) = a(\tau^n(x_1)) - a(\tau^n(x_0)). \qquad (4.11)$$

This quantity cannot grow for bounded initial a, and so the flux through an interval cannot grow in the case $\alpha = 0$. The behaviour of this projection depends sensitively on the endpoints as the map τ is chaotic. Except in this special case of $\alpha = 0$, it is not at all clear how to study the flux through intervals in the SFS map (see [14] and discussion in section 1.1 above).

5 Properties of T and T^* in L^2

In this section we consider spectral properties of the SFS operator T and its adjoint T^* acting on L^2, the space of square-integrable functions. Our aim is to understand their spectra, and ascertain when eigenfunctions exist and how smooth they are. We will find that T^* has many eigenfunctions, but these are not smooth, and so do not enable us to prove perfect dynamo action. Note that we have defined the growth rate $\gamma(\varepsilon)$ in (1.2) using energy and so this naturally has an L^2 setting. In paper II we will consider the effects of diffusion and how the L^2 spectrum with diffusion relates to that in paper I for $\varepsilon = 0$. Related results for spectra in Anosov flows and maps may be found in [24,25,35]. In this section we use $\|b\| = (b, b)^{1/2}$ as the L^2 norm and recall that the inner product defined makes L^2 a Hilbert space; we use $\perp$ to denote the orthogonal complement of a linear subspace. We have used as sources on linear functional analysis [9,20].

We begin by noting the kernels and images of T and T^*,

$$\operatorname{Ker} T = (\operatorname{Im} T^*)^\perp = \{0\}, \quad \operatorname{Ker} T^* = (\operatorname{Im} T)^\perp = \{b : e^{i\alpha x} b(x) \text{ is even}\}. \quad (5.1)$$

Thus $\lambda = 0$ is an eigenvalue of T^* with infinite degeneracy.

Recall that the spectrum of a general operator A is defined by

$$\sigma(A) = \{\lambda \in \mathbb{C} : \lambda I - A \text{ is not invertible}\}, \quad (5.2)$$

where invertibility includes the requirement that the inverse be bounded as an operator in L^2. The spectrum may be broken up into several components. For λ in the *point spectrum* $\sigma_{\mathrm{p}}(A)$ there are eigenvectors of A, $\operatorname{Ker}(\lambda I - A) \neq (0)$. For λ in the *approximate spectrum* $\sigma_{\mathrm{ap}}(A)$, $\lambda I - A$ is not bounded below, i.e., there does not exist $\epsilon > 0$ for which $\|(\lambda I - A)b\| \geq \varepsilon \|b\|$ for every b in L^2. Finally for λ in the *compression spectrum* $\sigma_{\mathrm{com}}(A)$, $\operatorname{Im}(\lambda I - A)$ is not dense in L^2. We have

$$\sigma_{\mathrm{p}}(A) \subset \sigma_{\mathrm{ap}}(A), \quad \sigma(A) = \sigma_{\mathrm{ap}}(A) \cup \sigma_{\mathrm{com}}(A). \quad (5.3)$$

For $\lambda \in \sigma_{\mathrm{ap}}(A)$, there exists an *approximate eigenfunction*, a sequence $b_{(n)}$ with

$$\|b_{(n)}\| = 1, \qquad \|(\lambda I - T)b_{(n)}\| \to 0 \quad \text{as} \quad n \to \infty \quad (5.4)$$

For $\lambda \in \sigma_{\mathrm{com}}(A)$ the set $\overline{\operatorname{Im}(\lambda I - A)}$ is a closed subspace of L^2, whose orthogonal complement, equal to $\operatorname{Ker}(\overline{\lambda} I - A^*)$, is non-zero. It follows that

$$\sigma_{\mathrm{com}}(A) = \operatorname{conj} \sigma_{\mathrm{p}}(A^*), \quad (5.5)$$

where 'conj' denotes complex conjugation of a set. It is usual also to define residual spectrum $\sigma_{\mathrm{r}} = \sigma_{\mathrm{com}} \setminus \sigma_{\mathrm{p}}$ and continuous spectrum by $\sigma_{\mathrm{c}} = \sigma \setminus (\sigma_{\mathrm{com}} \cup \sigma_{\mathrm{p}})$ so that $\sigma = \sigma_{\mathrm{p}} \cup \sigma_{\mathrm{c}} \cup \sigma_{\mathrm{r}}$ as a disjoint union. However we shall not make use of this as it is difficult to characterise σ_{p} precisely in our models.

The SFS operator T has the important property that $T/2$ is an *isometry*, $\|Tb\| = 2\|b\|$. This has the immediate consequence that $\gamma(0) = 2$ from (1.2). Also $\|T\| = \|T^*\| = 2$ and so $\sigma(T) = \operatorname{conj} \sigma(T^*)$ is a closed non-empty subset of the closed disc

$$\Delta = \{\lambda : |\lambda| \leq 2\}. \quad (5.6)$$

Another consequence of $T/2$ being an isometry is that the approximate spectrum $\sigma_{\mathrm{ap}} \subset \partial\Delta$, the circle $|\lambda| = 2$. This follows by noting that $\|(\lambda I - T)b\| \geq$

$(|\lambda| - 2)\|b\|$ and supposing there exists an approximate eigenfunction (5.4); this is only possible if $|\lambda| = 2$.

We also know that $0 \in \sigma_{\rm p}(T^*) = \operatorname{conj}\sigma_{\rm com}(T)$ by (5.1) and we have the general result that the boundary of the spectrum $\partial\sigma(T) \subset \sigma_{\rm ap}(T)$. It follows that $\sigma_{\rm ap}(T)$ must be non-empty and in fact must be the whole of $\partial\Delta$. We deduce that

$$\sigma(T) = \sigma_{\rm ap}(T) \cup \sigma_{\rm com}(T) = \Delta, \quad \sigma_{\rm ap}(T) = \partial\Delta. \tag{5.7}$$

For T^* we have

$$\sigma(T^*) = \sigma_{\rm ap}(T^*) = \Delta, \quad \sigma_{\rm p}(T^*) \supset \operatorname{Int}\Delta, \tag{5.8}$$

where 'Int' denotes the interior of a set. These results tell us much about the spectra of T and T^*. In particular T^* has many eigenfunctions: any λ with $|\lambda| < 2$ is an eigenvalue! However smoothness is the primary consideration for perfect dynamo action, and we do not know how smooth these eigenfunctions are; this we consider next. [1]

Another useful property of the SFS model is that $T^*T = 4I$ and so T^* has a right inverse $R = \frac{1}{4}T$ [12]. This means that if b is an eigenfunction of T with, necessarily, $|\lambda| = 2$, we have $Tb = \lambda b$, and applying T^* gives $T^*b = 4b/\lambda = \overline{\lambda}b$. Any eigenfunction of T with eigenvalue λ is an eigenfunction of T^* with eigenvalue $\overline{\lambda}$, and so

$$\sigma_{\rm p}(T) \subset \operatorname{conj}\sigma_{\rm p}(T^*). \tag{5.9}$$

Similarly if T has an approximate eigenfunction (5.4) with $(\lambda I - T)b_{(n)} \equiv d_{(n)} \to 0$ and necessarily $|\lambda| = 2$, then since $(\overline{\lambda}I - T^*)b_{(n)} = -T^*d_{(n)}/\lambda \to 0$, this equally provides an approximate eigenfunction for T^*. This also implies that $\sigma_{\rm ap}(T) \subset \operatorname{conj}\sigma_{\rm ap}(T^*)$, but we already know this.

The remaining issue is whether any points in $\sigma_{\rm p}(T)$ or $\sigma_{\rm p}(T^*)$ lie on the circle $\partial\Delta$. We can show that they do not for $\alpha = 0$, and so $\sigma_{\rm p}(T)$ is empty in this case. To prove this expand a possible eigenfunction as a series using the basis $\sin(\frac{1}{2}n\pi(x+1))$ or a Haar basis (e.g., [9,33]). On such a basis T doubles the wavenumber n and one can deduce that all the expansion coefficients are zero. We omit the details here (see section 9.5.3 of [12], paper II).

We cannot prove anything for general values of α; however the related models stretch–stack–fold (appendix A) and stretch–fold–slide [21,22] do have eigenfunctions of T for selected values of the shear α. Whether eigenfunctions of

[1] Note that sections 9.5.2 and 9.6.1 of [12] are incomplete here: these discuss smooth eigenfunctions analogous to those we consider in section 6 below, but not the rest of the L^2 spectrum.

T can exist or not appears to depend sensitively on the form of the phase function $f(x)$ used (see (2.11)) and in appendix B we show that for SFS with generic phase function f, the operator T has no continuous eigenfunctions. We also note that it is sometimes possible to interpret eigenfunctions of T in terms of distributions [12,28], but we do not pursue this line here.

5.2 Shift operators and eigenfunctions

In this section and the next we flesh out the above results on the spectrum of T and T^* by actually constructing eigenfunctions and approximate eigenfunctions, to better understand their properties. Now the operator T is analogous to a 'shift' operator moving fields into smaller scales by the stretch–fold operation. On the other hand T^* shifts structure into large scales. This analogy will be made more precise below but for the present consider simply the operators on sequences in l^2 given by

$$T_{\rm r}(a_0,a_1,a_2,\dots)=2(0,a_0,a_1,\dots),\quad T_{\rm r}^*(a_0,a_1,a_2,\dots)=2(a_1,a_2,a_3,\dots), \tag{5.10}$$

(twice) right and left shift operators respectively. Note that $T_{\rm r}^*T_{\rm r}=4I$ and so $T_{\rm r}^*$ has a right inverse $\frac{1}{4}T_{\rm r}$. For this standard example (e.g., p. 173 of [9]) we have

$$\sigma(T_{\rm r})=\sigma(T_{\rm r}^*)=\Delta,\quad \sigma_{\rm ap}(T_{\rm r})=\partial\Delta,\quad \sigma_{\rm ap}(T_{\rm r}^*)=\Delta, \tag{5.11}$$

$$\sigma_{\rm com}(T_{\rm r})=\sigma_{\rm p}(T_{\rm r}^*)=\mathrm{Int}\,\Delta,\quad \sigma_{\rm p}(T_{\rm r})=\sigma_{\rm com}(T_{\rm r}^*)=\emptyset. \tag{5.12}$$

Indeed, given any eigenvalue λ of $T_{\rm r}^*$ with $|\lambda|<2$, the corresponding eigenfunction is given by

$$c=(1,\lambda/2,\lambda^2/4,\lambda^3/8,\dots). \tag{5.13}$$

Also, given any approximate eigenvalue λ of $T_{\rm r}$ with $|\lambda|=2$, we may define a sequence of functions $b_{(n)}$ by

$$b_{(n)}=n^{-1/2}(1,2/\lambda,4/\lambda^2,\dots,2^{n-1}/\lambda^{n-1},0,0,\dots). \tag{5.14}$$

Here

$$\|b_{(n)}\|=1,\quad \|(\lambda I-T_{\rm r})b_{(n)}\|^2=8/n\to 0, \tag{5.15}$$

as $n\to\infty$. This explicit construction confirms that λ is an approximate eigenvalue of $T_{\rm r}$. This sequence also provides an approximate eigenfunction of $T_{\rm r}^*$ with eigenvalue $\overline{\lambda}$, analogous to discussion below (5.9).

Returning now to the SFS adjoint operator T^* we may construct eigenfunctions in a similar way. Recall that T^* has a right inverse $R = \frac{1}{4}T$, analogous to the situation for the shift maps in (5.10) above, and we can use the above constructions. First we construct an eigenfunction of T^*. Given any eigenvalue with λ, $|\lambda| < 2$ and an initial field $c_0 \in \operatorname{Ker} T^*$ we define the eigenfunction by

$$c = \sum_{n=0}^{\infty} \lambda^n R^n c_0. \tag{5.16}$$

This converges since $\|R\| = \frac{1}{2}$. This construction applies for any α, and we can choose $|\lambda| > 1$ to obtain a growing eigenfunction of T^*. This appears to contradict the discussion for $\alpha = 0$ in section 4.3, in which we showed that no growth could occur in $(T^{*n}c, b)$; see (4.10). However there we required that c be C^1, whereas here this is not guaranteed. We need to investigate the smoothness of an eigenfunction in more detail.

Plainly the eigenfunction (5.16) will not generally be continuous, let alone smooth, because of the piecewise definition of T_{SF} in (2.4). However if the initial field c_0 is chosen to be continuous and satisfy $c_0(-1) = c_0(1) = 0$ then $R^n c_0$ is continuous for all n. If we use a supremum norm, $\|R\|_\infty = \frac{1}{2}$ and the series converges uniformly to a continuous eigenfunction c.

We can go further than this and choose a smooth initial field c_0 such that all even derivatives $c_0^{(r)}(x)$, $r = 0, 2, \ldots$ vanish at $x = \pm 1$. For this class of initial conditions $R^n c$ remains smooth for all n and we can obtain for the nth derivative

$$\|(Rc)^{(r)}\|_\infty \leq \tfrac{1}{2} \sum_{m=0}^{r} \binom{r}{m} \alpha^{r-m} 2^m \|c^{(m)}\|_\infty. \tag{5.17}$$

This has the general structure

$$\|(Rc)^{(r)}\|_\infty \leq 2^{r-1} \|c^{(r)}\|_\infty + \text{lower order derivatives of } c, \tag{5.18}$$

and from this it may be checked that

$$\|(R^n c)^{(r)}\|_\infty = O((2^{r-1})^n) \qquad (n \to \infty) \tag{5.19}$$

(cf. [8]). Thus if $|\lambda| < 2^{1-r}$ the rth derivative converges uniformly in the sum (5.16) and the eigenfunction c so constructed is C^r.

Thus to summarise, we can easily construct a continous eigenfunction c of T^* for any $|\lambda| < 2$, but if we impose differentiability we have to restrict to decaying modes $|\lambda| < 1$ in our construction. This is in accord with our discussion about

the lack of amplification of $(c, T^n b)$ for a C^1 function c and $\alpha = 0$ in section (4.3) above. As we impose additional good behaviour the values of $|\lambda|$ are further restricted. For smooth, that is C^∞, eigenfunctions we are left with $\lambda = 0$, when there are plenty in the kernel of T^* (5.1). Of course this is not to say that there do not exist smooth eigenfunctions with $\lambda \neq 0$, indeed we shall find these for certain values of λ and α below, only that the above explicit construction does not help us.

We may also construct approximate eigenfunctions (5.4) for T and T^* following the construction (5.14) for the right shift operator. For any λ with $|\lambda| = 2$ we define a sequence of functions

$$b_{(n)} = n^{-1/2} \sum_{m=0}^{n-1} \lambda^{-m} T^m b_{(n)0}, \tag{5.20}$$

where for each n, we are free to choose the initial field $b_{(n)0}(x)$. Suppose we choose this initial field to have $\|b_{(n)0}\| = 1$ and to be localised, with support in a small neighbouhood of $x = 0$. Then $Tb_{(n)0}$ has field localised in neighbourhood of $x = \pm\frac{1}{2}$ and $T^2 b_{(n)0}$ in neighbourhoods of $x = \pm\frac{1}{4}, \pm\frac{3}{4}$, and so forth. For each n we can thus choose $b_{(n)0}$ so that the supports of iterates do not overlap,

$$(T^m b_{(n)0}, T^p b_{(n)0}) = 0 \qquad (0 \leq m < p \leq n). \tag{5.21}$$

It is then easy to check that

$$\|b_{(n)}\| = 1, \quad \|(\lambda I - T) b_{(n)}\|^2 = 8/n, \tag{5.22}$$

analogously to (5.15).

5.4 Lack of compactness in L^2 and normality

In order to make progress in finding smooth growing eigenfunctions, we will shortly restrict our attention to a smaller function space $\mathcal{B} \subset L^2$. In this space the restricted operator $S = T^*|_{\mathcal{B}}$ is compact and so has a discrete, point spectrum only. The operators T and T^* are not compact in L^2 (cf. [12]). To show this for T we exhibit a bounded sequence b_n for which the image sequence Tb_n has no convergent subsequence. Set

$$b_n = \sin \tfrac{1}{2} n\pi(x+1), \quad Tb_n = 2e^{-i\alpha x} \sin n\pi(x+1), \tag{5.23}$$

for which $\|Tb_n - Tb_m\| = 2\sqrt{2}$ for $n \neq m$. The lack of compactness of T^* is then a standard result (p. 159 of [20]).

Finally note that

$$(T^*T - TT^*)c(x) = 2c(x) + 2e^{-2i\alpha x} c(-x) \tag{5.24}$$

and so T is not normal in general, only on the subspace of functions for which $e^{i\alpha x}c(x)$ is odd, that is, $\mathrm{Im}\, T$ from (5.1).

6 Restriction to a space of analytic functions, $\mathcal{B}$

In the last section we gave a discussion of spectra of the direct stretch–fold–shear operator T and its adjoint T^* acting in L^2. We explicitly constructed continuous growing eigenfunctions of the adjoint operator T^* for any α, but this does not show perfect dynamo action because the eigenfunctions lack the required smoothness properties. The case $\alpha = 0$ highlights this: we showed in section 4.3 that $(c, T^n b)$ does not grow for any smooth c and b.

We are aiming to demonstrate perfect dynamo action, and we argued below (2.10) that because of the action of T^* (2.9) in stretching out structure, there should exist smooth eigenfunctions. But we have been unable to find them, except in a few cases (4.3,4.4) of marginal importance. What has gone wrong? Rather than yield smooth eigenfunctions, our explicit construction has given us eigenfunctions with structure on all scales; if one applies T^* structure simply passes up one scale.

From the dynamo point of view, these eigenfunctions with structure on all scales will not be robust to diffusion, which will strongly damp small scales. The effect of introducing weak diffusion $0 < \varepsilon \ll 1$ will in fact cause the spectrum of T to collapse to a discrete set (see paper II). This need for robustness to diffusion is the reason for the requirement of smoothness in the definition of a perfect dynamo (section 1.1). The problem in finding smooth eigenfunctions is that the space L^2 is too large for our purposes, and it is better to work in a more restricted space where smoothness is guaranteed. A result of [8] is relevant here: it is shown that starting with smooth initial conditions a field growing under T^*, when normalised has all derivatives bounded. Thus starting from smooth initial conditions, one cannot realise individual members of the large family of eigenfunctions we have constructed. Only a smaller set with good smoothness properties is likely to be relevant.

In this section we begin to seek smooth eigenfunctions of T^*. Our approach is to restrict the space of functions in which we work to a subset $\mathcal{B}$ of L^2 consisting of functions $c(z)$ that are analytic in a disc containing $[-1, 1]$. All functions in this subset are smooth, and although we cannot guarantee finding all smooth growing eigenfunctions, it is sufficient to find some in $\mathcal{B}$ to show that SFS is a perfect dynamo. We again use [9,20] as references. These techniques are well known in the dynamical systems literature; see, for example, [26,29].

6.1 *Definition of $\mathcal{B}$ and the operator S*

We fix a parameter $r > 1$ and let $\mathcal{B}$ be the space of complex functions analytic in the open disc $\mathcal{D} = \{z : |z| < r\}$ and continuous in the closed disc $\overline{\mathcal{D}}$, under the supremum norm,

$$\|c\| = \sup_{z \in \mathcal{D}} |c(z)|. \tag{6.1}$$

We take $\|\cdot\|$ to be this norm from now on, rather than the earlier L^2 norm. $\mathcal{B}$ is a Banach space as it is complete: a Cauchy sequence $c_{(n)}$ of continuous functions in $\mathcal{B}$ must converge uniformly to a continuous function c (as $\overline{\mathcal{D}}$ is compact). Since $c_{(n)}$ for each n satisfies Cauchy's integral formula, so must c, and differentiating this formula establishes that $c(z)$ is analytic in $\mathcal{D}$, as required.

Functions in $\mathcal{B}$ are automatically smooth on $[-1, 1]$ and so lie in L^2. We will therefore restrict T^* to $\mathcal{B}$ and consider the spectrum of the resulting operator; we call this operator $S = T^*|_{\mathcal{B}}$ (note we place no star on S), as it acts on a different space from T^* and so has different properties. We define the operators $S_{\mathrm{SF}} = T^*_{\mathrm{SF}}|_{\mathcal{B}}$ and $S_{\mathrm{Sh}} = T^*_{\mathrm{Sh}}|_{\mathcal{B}}$ in the same way from (2.10).

We have $S(\mathcal{B}) \subset \mathcal{B}$ and S is a bounded operator on $\mathcal{B}$. To show this first define

$$S_1 c(z) = c(\tfrac{1}{2}(z-1)), \quad S_2 c(z) = c(\tfrac{1}{2}(1-z)), \tag{6.2}$$

$$S_3 c(z) = e^{i\alpha z/2} c(z), \quad S_4 c(z) = e^{-i\alpha z/2} c(z), \quad S_{\mathrm{Sh}} c(z) = e^{i\alpha z} c(z), \tag{6.3}$$

so that

$$S = e^{-i\alpha/2} S_3 S_1 - e^{i\alpha/2} S_4 S_2 = (S_1 - S_2) S_{\mathrm{Sh}}. \tag{6.4}$$

Now suppose $c \in \mathcal{B}$. Then c is analytic in $\mathcal{D}$ and so $S_1 c$ and $S_2 c$ are analytic in the disc $|z - 1| < 2r$, which contains $\mathcal{D}$ given that $r > 1$. It is then clear that $Sc \in \mathcal{B}$. We also have

$$\|S_1\| = \|S_2\| = 1, \quad \|S_3\| = \|S_4\| = e^{\alpha r/2}, \quad \|S_{\mathrm{Sh}}\| = e^{\alpha r}, \tag{6.5}$$

(with equality if applied to a constant function) and thus

$$\|S\| \leq 2e^{\alpha r/2}. \tag{6.6}$$

6.2 *Compactness of S*

The fact that S is 'analyticity improving', mapping a function analytic in $\mathcal{D}$ to a function analytic in a larger disc, has the important implication that the

operator S is compact; if $c_{(n)}$ is a bounded sequence of functions in $\mathcal{B}$ then the sequence $Sc_{(n)}$ has a convergent subsequence. We give the proof below for completeness, using [9,26].

It is sufficient to show that the operators S_1 and S_2 are compact, since the composition of a bounded operator and a compact operator is compact. We consider only S_1 and let B be the unit ball in $\mathcal{B}$: S_1 is compact if S_1B is compact. By the Arzelà–Ascoli theorem it is sufficient to check that S_1B is bounded (which it is as S_1 is bounded) and equicontinuous. S_1B is *equicontinuous*, if given any $z \in \overline{\mathcal{D}}$ and ε, there is neighbourhood $U_z \subset \overline{\mathcal{D}}$ of z such that for all $z_1 \in U_z$ and $c \in B$, we have $|S_1c(z) - S_1c(z_1)| < \varepsilon$.

To show that S_1B is equicontinuous, let $z \in \overline{\mathcal{D}}$ and $c \in B$. We may use Cauchy's integral formula, as $(z-1)/2$ lies inside $\mathcal{D}$,

$$S_1c(z) = \frac{1}{2\pi i}\oint_{|w|=r} \frac{c(w)}{w - \frac{1}{2}(z-1)}\,dw. \tag{6.7}$$

Thus applying this also for $z_1 \in \overline{\mathcal{D}}$,

$$S_1c(z) - S_1c(z_1) = \frac{1}{2\pi i}\oint_{|w|=r} \frac{c(w)\frac{1}{2}(z-z_1)}{(w - \frac{1}{2}(z-1))(w - \frac{1}{2}(z_1-1))}\,dw. \tag{6.8}$$

Now $|\frac{1}{2}(z-1)| \leq \frac{1}{2}(r+1)$ as $|z| \leq r$ and so $|w - \frac{1}{2}(z-1)| \geq \frac{1}{2}(r-1)$ (as $|w| = r$). This yields

$$|S_1c(z) - S_1c(z_1)| \leq \|c\|\,|z - z_1|\,2r(r-1)^{-2}. \tag{6.9}$$

This bound is enough to establish equicontinuity of S_1B and so compactness of S.

The fact that S is compact is a key simplification; we recall that the original operator T^* on L^2 does not have this property (section 5.4). Since S is compact, it has only point spectrum, $\sigma(S) = \sigma_{\mathrm{p}}(S)$, and this is a countable set with no accumulation point different from zero. Each point λ in the spectrum is an eigenvalue of S with finite multiplicity; this also corresponds to an eigenvalue of the original operator T^* on L^2 with a smooth eigenfunction.

We cannot say a great deal more about general eigenfunctions and we need to approximate S to find these, as we discuss in the next section. Examples of such eigenfunctions are (4.3,4.4). Here we only note that any eigenfunction c of S with non-zero eigenvalue λ must be entire. For c is analytic in $|z| < r$, and so Sc is analytic in $|z-1| < 2r$ which includes the disc $|z| < 2r-1$. Generally S^nc is analytic in the disc $|z| < 1 + 2^n(r-1)$. But $c = \lambda^{-n}S^nc$ and the result follows. This result is important as it indicates that any choice of $r > 1$ would yield the same eigenfunctions and eigenvalues; r is a parameter at

our disposal. In fact we could use any neighbourhood of $[-1,1] \subset \mathbb{C}$ to define $\mathcal{B}$, rather than a disc. Also the above discussion goes through for a general phase function f (see (2.11)) provided that f is itself in $\mathcal{B}$, when αr is replaced by $\|f\|$ in the above estimates.

6.3 The adjoint space $\mathcal{B}^*$

It is useful also to consider the adjoint S^* of S and how it acts. This will become important in paper II, when we will study weak diffusion using perturbation theory and will need adjoint eigenfunctions to implement solvability conditions. At first sight, as S arose from restricting T^* to $\mathcal{B} \subset L^2$, this suggests we must reconsider T itself. However this is not the case; S^* bears little immediate relationship to T. We follow [29] here.

First consider again the space $\mathcal{B}$ which has a basis of unit vectors,

$$e_n(z) = r^{-n} z^n. \tag{6.10}$$

If we expand a complex function $c \in \mathcal{B}$ as a Taylor series [2]

$$c(z) = \sum_{n=0}^{\infty} c_n z^n, \tag{6.11}$$

then we have

$$r^n |c_n| \leq \|c\| \leq \sum_{n=0}^{\infty} r^n |c_n| \tag{6.12}$$

The left-hand side is obtained by Cauchy's integral formula, the right-hand side from (6.1). We note that we cannot easily specify $\|c\|$ in terms of the coefficients c_n, nor which sequences of coefficients $\{c_n\}$ correspond to functions c in $\mathcal{B}$. Equation (6.12) is the best we can do, and even here it may be possible for the right-hand side to be infinite and so give no information on $\|c\|$. Note however that eigenfunctions of S are entire, the coefficients in (6.11) thus go rapidly to zero, and so (6.12) will give us useful information.

We then consider the adjoint space $\mathcal{B}^*$, that is the space of bounded linear forms $\mathcal{B} \to \mathbb{C}$. If b is a form in $\mathcal{B}^*$ then we write $\langle b, c \rangle$ for its action on c; note that $\langle \cdot, \cdot \rangle$ is bilinear, unlike the original L^2 inner product (1.3). The norm in

[2] Note that this Taylor series need not converge on the boundary of $\mathcal{D}$; however it will converge on any closed disc inside $\mathcal{D}$ and knowledge of the coefficients c_n is sufficient completely to specify a given function $c \in \mathcal{B}$.

$\mathcal{B}^*$ is given by

$$\|b\| = \sup_{c\in\mathcal{B},\,\|c\|=1} |\langle b, c\rangle|. \tag{6.13}$$

The adjoint basis to e_n is e_n^* with

$$\langle e_n^*, c\rangle = \frac{1}{2\pi i}\oint_{\partial\mathcal{D}} \frac{r^n}{z^{n+1}}\, c(z)\, dz. \tag{6.14}$$

A general form b in $\mathcal{B}^*$ may be written as a sum of these basis vectors. With some abuse of notation we may identify a basis form with a function

$$e_n^*(z) = r^n z^{-n-1} \tag{6.15}$$

and identify a general form b with a function

$$b(z) = \sum_{n=0}^{\infty} b_n z^{-n-1}, \tag{6.16}$$

which acts on $c \in \mathcal{B}$ via

$$\langle b, c\rangle = \frac{1}{2\pi i}\oint_{\partial\mathcal{D}} b(z)c(z)dz = \sum_{n=0}^{\infty} b_n c_n. \tag{6.17}$$

Plainly

$$r^{-n}|b_n| \le \|b\| \le \sum_{n=0}^{\infty} r^{-n}|b_n|. \tag{6.18}$$

Thus the function $b(z)$ in (6.16) identified with a general form b, vanishes at infinity and is analytic in $\mathcal{D}^* = \mathbb{C}^*\backslash\overline{\mathcal{D}}$, where $\mathbb{C}^* = \mathbb{C}\cup\{\infty\}$ is the extended complex plane. Again, however, we cannot precisely specify $\|b\|$ in terms of $\{b_n\}$, and the right-hand side of (6.18) may be infinite and so give no information.

Note that we have not included r in the definition of the series (6.16) and (6.11) for b and c. It is convenient not to do this, as the actual eigenfunctions we find do not depend on the choice of r. We also note in passing that if we have an operator such as S, on $\mathcal{B}$ with matrix elements $A_{mn} = \langle z^{-m-1}, Sz^n\rangle = r^{n-m}\langle e_m^*, Se_n\rangle$ (as we use in (3.3)) then the norm of S is bounded by

$$\|S\| \le \sum_{m,n} |\langle e_m^*, Se_n\rangle| = \sum_{m,n} r^{m-n}|A_{mn}|. \tag{6.19}$$

We will use this bound below. The matrix elements A_{mn} for the adjoint SFS operator S are given back in equation (3.3) and fall off geometrically as either n or m is increased; it may be shown that

$$r^{m-n}|A_{mn}| \le 2e^{\alpha r/2}\left(\frac{r+1}{2r}\right)^n, \quad r^{m-n}|A_{mn}| \le 4e^{\alpha r}\left(\frac{r}{2r-1}\right)^{m+1}; \tag{6.20}$$

see similar calculations in sections 7.3 and 7.4 below. It is this geometrical fall-off in matrix coefficients [3,29] that will allow us to approximate S by a finite matrix below. It is also why zeta function methods work in obtaining growth rates using periodic orbit sums in SFS and similar fast dynamo models [1–5,29].

6.4 The adjoint operator S^*

Now we have defined the adjoint space $\mathcal{B}^*$, we can obtain the adjoint operator S^* to S, defined using (6.17) by

$$\langle S^*b, c\rangle = \langle b, Sc\rangle = \frac{1}{2\pi i}\oint_{\partial\mathcal{D}} b(z)[e^{i\alpha\frac{1}{2}(z-1)}c(\tfrac{1}{2}(z-1)) - e^{i\alpha\frac{1}{2}(1-z)}c(\tfrac{1}{2}(1-z))]\,dz, \tag{6.21}$$

so that, changing variables in the integration,

$$(2\pi i)\langle S^*b, c\rangle = \oint_{|1+2z|=r} 2b(1+2z)e^{i\alpha z}c(z)\,dz + \oint_{|1-2z|=r} 2b(1-2z)e^{i\alpha z}c(z)\,dz. \tag{6.22}$$

Now $c(z)$ is analytic inside $\mathcal{D}$, that is inside $|z| = r$, while $b(1+2z)$ is analytic outside the circle $|1+2z| = r$, which lies inside $\mathcal{D}$. We can therefore distort the contour in the first integral (and similarly the second) back to $\partial\mathcal{D}$ to give

$$\langle S^*b, c\rangle = \frac{1}{2\pi i}\oint_{\partial\mathcal{D}} 2e^{i\alpha z}[b(1+2z) + b(1-2z)]c(z)\,dz. \tag{6.23}$$

This gives S^*b in the form of an integral, and we wish to identify this with a complex function of the form (6.16). To do this we project out all positive or zero powers to leave

$$S^*b(z) = P_{\mathcal{B}^*}(2e^{i\alpha z}[b(1+2z) + b(1-2z)]), \tag{6.24}$$

where $P_{\mathcal{B}^*}$ denotes this projection.

Like the operator S, the adjoint operator S^* is analyticity improving. Suppose $b \in \mathcal{B}^*$ and so $b(z)$ is analytic in $\mathcal{D}^*$. Put

$$\phi_1(z) = 1+2z, \quad \phi_2(z) = 1-2z. \tag{6.25}$$

Then $b(\phi_1(z))$ is analytic in $|\phi_1(z)| > r$ or $|z+1/2| > r/2$. Similarly $b(\phi_2(z))$ is analytic in $|z-1/2| > r/2$. So S^*b is analytic in the intersection of these two regions, i.e., outside both of these circles. Similarly $S^{*n}b$ is analytic in

$$\{\infty\} \cup \bigcap_{m=0}^{2^n-1} \{z : |2^n(z+1) - 2m - 1| > r\}. \tag{6.26}$$

For an eigenfunction with non-zero eigenvalue, $b = \lambda^{-n} S^{*n} b$ for any n, and so taking the limit $n \to \infty$, is analytic in

$$\mathbb{C}^* \backslash [-1, 1]. \tag{6.27}$$

Generally eigenfunctions of S^* will be singular in this interval, and in the power series representation (6.16) the coefficients b_n need not tend to zero.

We do not have much more information about S^* and its eigenfunctions. We do not know of an explicit form for the adjoint eigenfunction corresponding to (4.3), but corresponding to direct eigenfunctions c_j in (4.4) we have adjoint eigenfunctions b_j with

$$b_j(z) = (z-1)^{-2j-1} - (z+1)^{-2j-1}, \quad \lambda = 2^{-2j} \qquad (\alpha = 0). \tag{6.28}$$

These satisfy $\langle b_j, c_k \rangle = 2j! \delta_{jk}$. The functions b_j have poles at the endpoints of $[-1, 1]$; related generalised eigenfunctions of T have been constructed with delta functions at these end points [12,28]. Whether other eigenfunctions of S^* may be related to generalised eigenfunctions of T remains an open question.

7 Perturbation theory for S in $\mathcal{B}$

We have set up a suitable framework in which to discuss S and S^*. They are compact operators and so we need only seek isolated eigenvalues with finite multiplicity. To do this we will use perturbation theory. The aim is to approximate S by a finite rank operator S_N whose eigenvalues may be computed numerically. Here N is an integer giving the level of truncation, and we may set $S = S_N + S'$. For us it makes sense to truncate power series to polynomials of degree $N - 1$.

7.1 Resolvents and pseudospectra

Before defining S_N we discuss approximations in general. Given a bounded operator A we may define the resolvent operator of A by $R_A(\zeta) = (\zeta I - A)^{-1}$, where ζ ranges over the complex plane. $R_A(\zeta)$ is defined and bounded except when ζ lies in the spectrum $\sigma(A)$. The basic result we need (p. 208 of [20]) is that if B is another bounded operator with norm μ, the spectrum of $A + B$ lies in the set defined by

$$\Lambda_\mu(A) = \{\zeta : \|R_A(\zeta)\| \geq \mu^{-1}\}. \tag{7.1}$$

This set is known as the μ-pseudospectrum of A [34]; it contains $\sigma(A)$ and generally has a number of components in the complex plane. In our case S

and S_N are compact operators, and the spectrum contains only of eigenvalues (accumulating nowhere except perhaps at zero) which move continuously under perturbation (see p. 213 of [20]). We suppose that

$$\|S'\| \to 0 \quad \text{as} \quad N \to \infty, \tag{7.2}$$

which we will verify below.

Consider first the case $A = S$. Given a non-zero eigenvalue of S, for sufficiently small μ this will be the only eigenvalue lying in a certain component of $\Lambda_\mu(S)$. We take N sufficiently large that $\|S'\| \leq \mu$. If we then take $B = -tS'$ and increase t from 0 to 1 it is clear that $S_N = S - S'$ will also have an eigenvalue in Λ_μ. Thus any given non-zero eigenvalue of S will be increasingly well approximated by an eigenvalue of S_N as $N \to \infty$. To check that our numerical results for a given eigenvalue converge correctly in this limit, we need only verify (7.2).

We can go further though, and use pseudo-spectra to place error bounds on numerical calculations. We now set $A = S_N$ and $B = tS'$ and increase t from 0 to 1: if S_N has an eigenvalue λ lying in a component of $\Lambda_\mu(S_N)$ with $\mu = \|S'\|$, then S must have an eigenvalue in the same component. We shall use this below in section 7.5 to give graphical error bounds on eigenvalues found numerically.

7.2 Definition of S_N

We now define the truncated, finite rank operator S_N. In view of the definition of $\mathcal{B}$ the natural procedure is to project a function $c(z)$ on its terms up to z^{N-1} in its Taylor series. We define a projection P to do this. It may be given by

$$Pc(z) = P\sum_{n=0}^{\infty} c_n z^n = \sum_{n=0}^{N-1} c_n z^n = \sum_{n=0}^{N-1} \langle e_n^*, c\rangle e_n(z), \tag{7.3}$$

or equivalently,

$$Pc(z) = \frac{1}{2\pi i}\oint_{\partial\mathcal{D}} \frac{1-(z/w)^N}{w-z}\, c(w)dw, \quad (I-P)c(z) = \frac{1}{2\pi i}\oint_{\partial\mathcal{D}} \frac{(z/w)^N}{w-z}\, c(w)dw. \tag{7.4}$$

We set $S_N = PS$ which maps $\mathcal{B}$ to the subspace $\mathcal{B}_N$ of polynomials of order $N-1$. To seek an eigenfunction c of S_N with non-zero eigenvalue λ, we need only consider $c \in \mathcal{B}_N$, in which case we are left with obtaining eigenvalues of the finite N by N matrix with entries A_{mn} defined in (3.3). Eigenfunctions and eigenvalues may now be found numerically. Eigenvalues are shown in figure

2(a) for $N = 128$ (solid) and $N = 64$ (dotted), while figure 4 shows leading eigenfunctions as functions of real z for $\alpha = 2$ and $\alpha = 10$. These are obtained from the right eigenvectors of A_{mn} and using (6.11) to reconstruct a polynomial in $\mathcal{B}_N$. Left eigenvectors give approximate adjoint eigenfunctions which may be identified with complex functions using (6.16), but it is not particularly illuminating to plot these.

7.3 Estimates of $\|S'\|$

As discussed above we need to check that $\|S'\|$ tends to zero as $N \to \infty$, where $S' = (I - P)S$. Recall the breaking up of the operator $S = (S_1 - S_2)S_{\mathrm{Sh}}$ defined in (6.2–6.4) above; we focus on the first term $S_1 S_{\mathrm{Sh}}$ as inclusion of the second term gives only an overall factor 2. First consider

$$(I - P)S_1 c(z) = \frac{1}{2\pi i} \oint_{\partial \mathcal{D}} \frac{(z/w)^N}{w - z} c(\tfrac{1}{2}(w - 1))\, dw. \tag{7.5}$$

Now we may push the contour out to $|w - 1| = 2r$ and note that $|z/w| \leq r/(2r - 1)$ and $|w - z| \geq r - 1$ since $|z| \leq r$. These inequalities give

$$\|(I - P)S_1\| \leq \frac{2r}{r - 1} \left(\frac{r}{2r - 1}\right)^N \equiv F_1(N). \tag{7.6}$$

Since $\|S_{\mathrm{Sh}}\| \leq e^{\alpha r}$ we are left with

$$\|S'\| \leq 2F_1(N)e^{\alpha r}. \tag{7.7}$$

For any given values of α and r, $\|S'\| \to 0$ as $N \to \infty$ and so the convergence of eigenvalues using the power series approximation (with results in figure 2(a)) is guaranteed, following the discussion in section 7.1. The geometrical reduction in norm is in accord with [29] and is a result of the hyperbolic stretching in the baker's map. Note that our estimates become poorer as the shear parameter α is increased. Also they depend on r, which is a parameter still at our disposal.

7.4 Error estimates for eigenvalues of S

We have established the convergence of the power series discretisation of the SFS adjoint operator S defined in the space $\mathcal{B}$. We wish to go further than this and establish error bounds on the eigenvalues found numerically for S_N with given values of N. There are two reasons for this. The first is to demonstrate convincingly that there is perfect dynamo action in the SFS model for given

values of α. This is worthwhile as little is known about perfect dynamo action, and SFS is the key model to study and generalise. Having said this we still rely on numerical computations and present error bounds graphically. The point is that the calculations will now involve finite values of N, rather than what we have so far, which is only the somewhat nebulous property of convergence in the limit $N \to \infty$.

Secondly we wish to establish error bounds to ensure that we understand the SFS model mathematically in as much depth as possible. It is not obvious at the outset that we can successfully establish error bounds. We know that for any given values of α and r there will be eigenvalues of S in the connected components of the pseudospectrum (7.1) of S_N with $\mu = \|S'\|$,

$$\Lambda_N \equiv \Lambda_\mu = \{\zeta : \|R_N(\zeta)\| \geq \mu^{-1}\} \qquad (R_N \equiv R_{S_N}, \mu = \|S'\|). \tag{7.8}$$

The problem is: how do we estimate $\|S'\|$ and $\|R_N(\zeta)\|$? Below we will be able to give only upper bounds $G(N)$ (7.21) on $\|S'\|$, and $H_N(\zeta)$ (7.24) on $\|R_N(\zeta)\|$. So we will be able only to plot the sets

$$L_N = \{\zeta : H_N(\zeta) \geq G(N)^{-1}\} \supset \Lambda_N. \tag{7.9}$$

It is possible that these bigger sets may not give any useful bounds on the location of eigenvalues in $\mathbb{C}$. If this is the case then we will not mathematically have established a tight enough grip on perfect dynamo action in the SFS model.

To establish error bounds it is convenient to redefine S_N, and we take

$$S_N = PSP, \quad S' = S - PSP. \tag{7.10}$$

S_N is totally defined by the square $N \times N$ matrix with entries A_{mn} in (3.3), and has the same eigenfunctions as the S_N defined earlier in section 7.2 (although eigenfunctions of the two operators S_N^* differ). We may write equally well

$$S' = (I - P)S + PS(I - P), \tag{7.11}$$
$$S' = (I - P)SP + S(I - P). \tag{7.12}$$

We again need to find $\|S'\|$ with this new definition of S'. We recall the decomposition of the operator S defined in (6.4) above. Consider

$$S_1(I - P)c(z) = \frac{1}{2\pi i} \oint_{\partial \mathcal{D}} \frac{((z-1)/2w)^N}{w - \frac{1}{2}(z-1)}\, c(w)\, dw. \tag{7.13}$$

Since $|z| \leq r$ we have $|(z-1)/2w| \leq (r+1)/2r$ and $|w - \frac{1}{2}(z-1)| \geq \frac{1}{2}(r-1)$,

and so we obtain

$$\|S_1(I-P)\| \leq \frac{2r}{r-1}\left(\frac{r+1}{2r}\right)^N \equiv F_2(N) \tag{7.14}$$

Noting that $\|P\| \leq N$ from (7.3) and recalling (6.4), (6.5) and (7.6), we have from (7.11)

$$\begin{aligned}
\|S'\| &\leq 2\|(I-P)S_1S_{\mathrm{Sh}}\| + 2\|PS_3S_1(I-P)\| && (7.15)\\
&\leq 2\|(I-P)S_1\|\|S_{\mathrm{Sh}}\| + 2\|P\|\|S_3\|\|S_1(I-P)\| && (7.16)\\
&\leq 2F_1(N)e^{\alpha r} + 2NF_2(N)e^{\alpha r/2} \equiv G_1(N), && (7.17)
\end{aligned}$$

or alternatively using (7.12),

$$\begin{aligned}
\|S'\| &\leq 2\|(I-P)S_1S_{\mathrm{Sh}}P\| + 2\|S_3S_1(I-P)\| && (7.18)\\
&\leq 2\|(I-P)S_1\|\|S_{\mathrm{Sh}}\|\|P\| + 2\|S_3\|\|S_1(I-P)\| && (7.19)\\
&\leq 2NF_1(N)e^{\alpha r} + 2F_2(N)e^{\alpha r/2} \equiv G_2(N). && (7.20)
\end{aligned}$$

We finally set

$$G(N) = \min(G_1(N), G_2(N)) \tag{7.21}$$

as the tightest estimate of the norm of S'.

We now need an estimate for the norm of $R_N(\zeta) = (\zeta I - S_N)^{-1}$. We have the matrix entries A_{mn} in (3.3) for $S_N : \mathcal{B} \to \mathcal{B}_N$. We restrict S_N to the subspace $\mathcal{B}_N \subset \mathcal{B}$, and on this space compute its resolvent by

$$\tilde{R}_N(\zeta) = (\zeta I_N - S_N)^{-1}, \tag{7.22}$$

where $I_N = P$ is the identity on $\mathcal{B}_N$. We then extend $\tilde{R}_N(\zeta)$ to the rest of $\mathcal{B}$ by defining it to be zero on z^n, $n \geq N$. Then it may be seen that the resolvent R_N of S_N on the full space $\mathcal{B}$ is given by

$$R_N(\zeta)c = \tilde{R}_N c + \zeta^{-1}(I-P)c = (\tilde{R}_N - \zeta^{-1}I_N)c + \zeta^{-1}c, \tag{7.23}$$

whence

$$\|R_N(\zeta)\| \leq \|\tilde{R}_N - \zeta^{-1}I_N\| + |\zeta|^{-1}. \tag{7.24}$$

Now to use this result, we can apply the upper bound (6.19) to $\|\tilde{R}_N - \zeta^{-1}I_N\|$ to give as an upper bound on $\|R_N(\zeta)\|$, which we will call $H_N(\zeta)$. This we can compute numerically as detailed next.

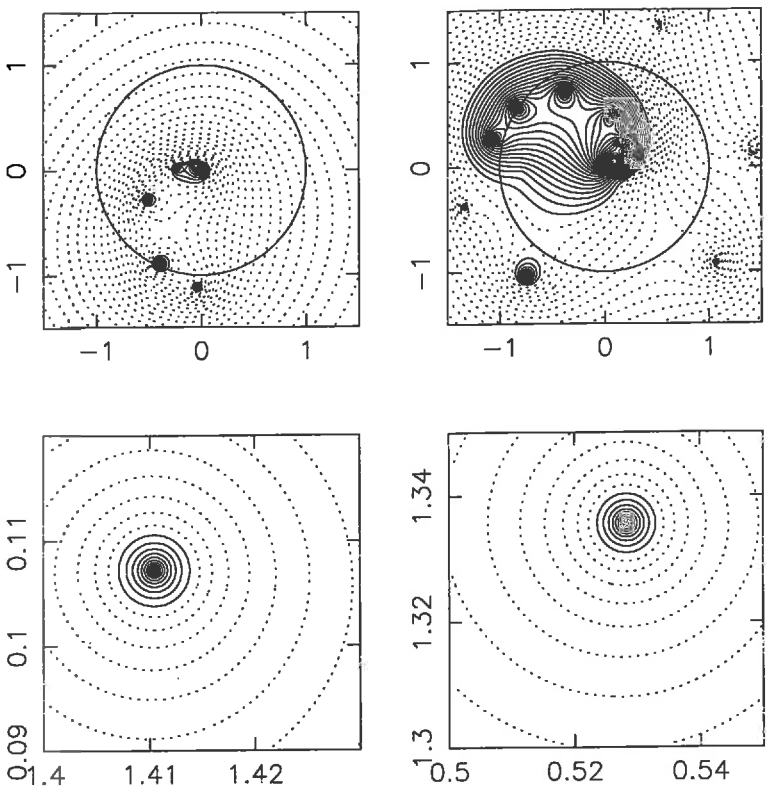

Fig. 5. Eigenvalues in the complex plane. Contour lines for $\log l_N(\eta)$ as a function of ζ are plotted in the complex plane for (a) (top left) $\alpha = 2$, $r = 2$, $N = 44$ and (b) (top right) $\alpha = 10$, $r = 2$ and $N = 116$. (c,d) show magnified regions of case (b). In each case dotted lines show regions in which $l_n < 1$ and solid lines $l_n \geq 1$; in the solid islands, eigenvalues are localised. The unit circle is also plotted in (a,b).

7.5 Numerical results and contour plots

We now have all the tools we need to isolate eigenvalues in the complex plane and to give error estimates, by means of contour plots. We set

$$l_N(\zeta) = H_N(\zeta)G(N), \tag{7.25}$$

so that the set L_N is given by $l_N(\zeta) \geq 1$. We take $r = 2$, as we have found little advantage in adjusting this parameter, and some given value of N. It is then straightforward to compute $G(N)$ from (7.21). To calculate $H_N(\zeta)$ we first set up the $N \times N$ matrix with entries A_{mn} defined in (3.3). This gives S_N and we may use a NAG matrix inversion routine to calculate $\tilde{R}_N(\zeta)$ from (7.22). We then use (7.24) together with (6.19) to compute numerically the upper bound $H_N(\zeta)$ on $\|R_N(\zeta)\|$. This is done for each value of ζ on a grid, and the results are shown as contour plots.

We have taken some illustrative values. Figure 5(a) shows a contour plot of $\log l_N(\zeta)$ for $r = 2$, $\alpha = 2$ and $N = 44$; in this case $G(N) = G_2(N) =$

5.3×10^{-4}. The distance between contours is $\frac{1}{4}$, and positive or zero contours are shown solid, negative contours dotted. Thus regions of the set L_N are indicated by the solid contours. The leading eigenvalues of the approximate operator S_N in this case are given by $\lambda_0 = -0.048 - i1.135$, $\lambda_1 = -0.416 - i0.909$ and the corresponding eigenfunctions are shown in figure 4(a,b). It may be seen that there are islands of L_N containing these values, and so the full operator S has an eigenvalue in these islands. In particular we note that the component containing the leading eigenvalue λ_0 is localised outside the unit circle; thus we conclude that there is an eigenvalue of S outside the unit circle, and so perfect dynamo action in the SFS model with $\alpha = 2$. The second eigenvalue λ_1 is simply the exact solution (4.3).

As another example figure 5(b) shows a similar contour plot for $r = 2$, $\alpha = 10$ and $N = 116$, for which $G(N) = G_2(N) = 2.3 \times 10^{-9}$. The leading eigenvalues of the approximate operator S_N are $\lambda_0 = 0.528 + i1.335$, $\lambda_1 = 1.410 + i0.107$, $\lambda_2 = -1.355 - i0.390$, $\lambda_3 = 1.053 - i0.932$, $\lambda_4 = -0.761 - i1.047$, $\lambda_5 = -1.065 + i0.266$ and $\lambda_6 = -0.839 + i0.544$. The corresponding eigenfunctions are shown in figure 4(c–k). The eigenvalues λ_0 to λ_4 lie in distinct components of L_N lying outside the unit circle; enlargements of figure 5(b) are shown in figure 5(c, d) to confirm this for λ_0 and λ_1. The corresponding eigenvalues of S are localised outside the unit circle, corresponding to perfect fast dynamo action with (at least) five modes destabilised. The eigenvalue λ_5 lies outside the unit circle, but the shape of the set L_N shown in figure 5(b) is such that we cannot isolate a corresponding eigenvalue of S outside the unit circle, at least for this value of N. The eigenvalue λ_6 is the exact solution (4.3).

We find that eigenvalues and estimates of $H_N(\zeta)$ obtained numerically appear to be relatively insensitive to N as N increases, whereas the term $G(N)$ decreases geometrically, and it is this that serves to give rapidly decreasing error bounds as N is increased.

8 Miscellaneous topics

8.1 Results for large shears

We recall that figure 2(a) shows results for $0 \leq \alpha \leq 10$ using the power series truncation, which we have justified mathematically. It is interesting to see what occurs for larger values of α. Using resolutions of 128^2 we can increase α to about 20 using the power series discretisation. However using the sine series discretisation (see figure 2(c)) we can increase α to about 40. Now while the sine series discretisation is poor for $|\lambda| \leq 1$ it agrees extremely well with the power series discretisation for larger λ.

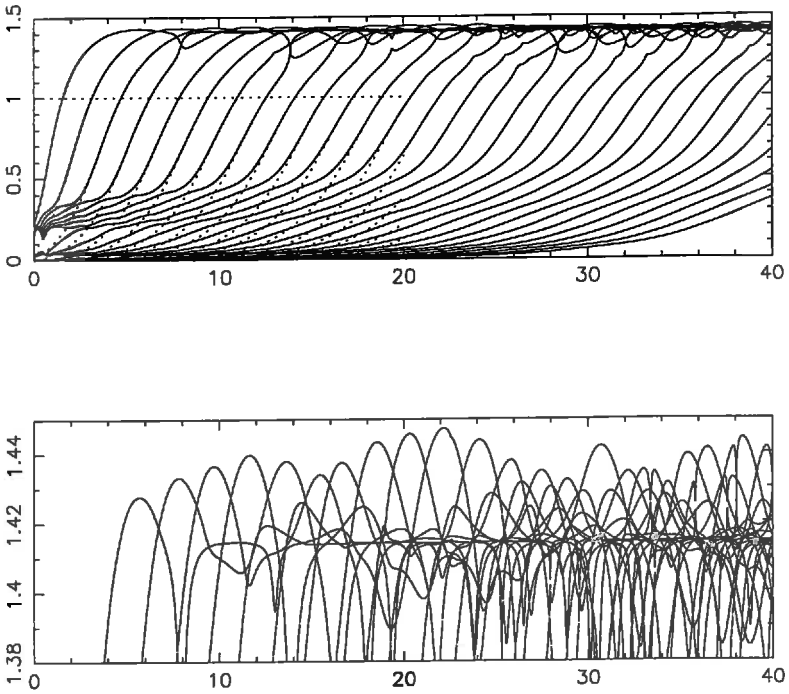

Fig. 6. Computations of eigenvalues λ of S. Absolute values $|\lambda|$ are plotted against α using the sine series discretisation (solid) and the power series discretisation (dotted) using matrices of size 128×128 (solid). (b) shows an enlargement of (a). Only the first thirty eigenvalues, ordered in modulus, are plotted and the resolution in α is 0.01.

In figure 6 we therefore show the power series discretisation (dotted) for $0 \leq \alpha \leq 20$ and the sine series discretisation (solid) for $0 \leq \alpha \leq 40$. Figure 6(b) shows an enlargement of 6(a). In this enlargement the two numerical methods give the same results for $0 \leq \alpha \leq 20$, and so the sine series results for larger α are likely to be correct even though we have no formal justification for this. On this assumption, we see that the individual branches appear to asymptote to a value of $\sqrt{2}$, in agreement with random-phase arguments of [22,28]. However the peaks appear to exceed this value as α is increased, and it appears that the perfect dynamo growth rate is greater than this value for any $\alpha > 5$, say.

8.2 Conjugacy

In this section we consider the SFS model but with a general phase function f as in (2.11), rather than linear f as we have considered so far. We explore briefly how eigenvalues depend on the form of f, working with S and taking $f \in \mathcal{B}$.

First we note that two distinct phase functions f and h may be related so as to give precisely the same eigenvalues; we refer to these as conjugate phase functions. Suppose we have a phase function f for which S_f has an eigenfunc-

tion c, $S_f c = \lambda c$, where we make the role of f explicit by means of a subscript. This can be written in the form

$$\lambda c(1+2x) = e^{-if(x)}c(x) - e^{-if(-x)}c(-x). \tag{8.1}$$

If we replace

$$c(1+2x) = e^{-ig(x)}d(1+2x), \quad \lambda = e^{-i\psi}\mu, \tag{8.2}$$

where $g(x)$ is an even function and ψ a constant, then we find that d is an eigenfunction of S_h, eigenvalue μ, where

$$h(x) = -g(x) + f(x) + g(\tfrac{1}{2}(x-1)) - \psi. \tag{8.3}$$

The eigenvalues will be unchanged in modulus, $|\lambda| = |\mu|$ under this change of phase function, or conjugacy of SFS models.

We can use this transformation to simplify phase functions. For example, a quadratic phase shift is equivalent to a linear phase shift, via,

$$f(x) = \alpha x + \beta x^2, \quad g(x) = 4\beta x^2/3, \quad \psi = \beta/3, \quad h(x) = (\alpha - 2\beta/3)x. \tag{8.4}$$

Clearly such conjugacy may be used to eliminate all even powers in a polynomial form of f.

In fact any f in $\mathcal{B}$ (for large enough r) is conjugate to a phase function which is odd. Let $f = f_{\text{even}} + f_{\text{odd}}$ and set $g = f_{\text{even}}$ and $\psi = f_0$, the constant term in f. The new phase function h is given by (8.3) above and, using obvious notation, satisfies

$$h_{\text{even}}(x) = P_{\text{even}}(f_{\text{even}}(\tfrac{1}{2}(x-1)) - f_0), \tag{8.5}$$
$$h_{\text{odd}}(x) = f_{\text{odd}}(x) + P_{\text{odd}}(f_{\text{even}}(\tfrac{1}{2}(x-1)) - f_0). \tag{8.6}$$

It may then be verified that

$$\|h_{\text{even}}\| \le C\|f_{\text{even}}\|, \quad \|h_{\text{odd}}\| \le \|f_{\text{odd}}\| + C\|f_{\text{even}}\|, \tag{8.7}$$

with $C = (r+1)^2/(4r^2 - (r+1)^2)$, and so for large enough r ($r > 1+\sqrt{2}$), the even part h_{even} has smaller norm than f_{even}. Iterating this process leads to convergence to a phase function in $\mathcal{B}$ which is odd and conjugate to the original f.

So we may consider just odd phase functions. These can give different results from linear shear. Consider the case when $f(x) = \alpha x^q$ for an integer q. Writing $S = S_{\text{SF}}S_{\text{Sh}}$ as usual, the non-zero matrix elements A_{mn} and B_{mn} in the power series representation for S_{SF} and S_{Sh} are

$$A_{mn} = (-1)^{m+1}2^{1-n}\frac{n!}{m!(n-m)!} \qquad (n \ge m, n \text{ odd}) \tag{8.8}$$

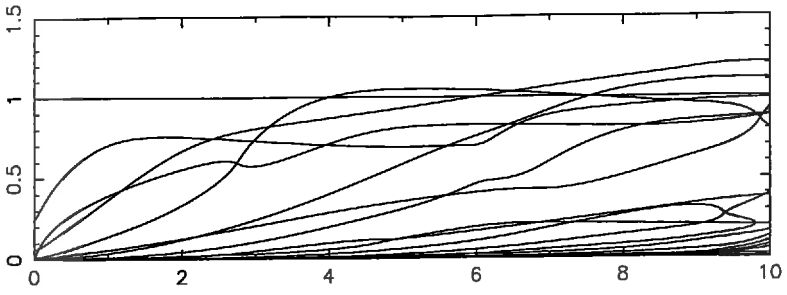

Fig. 7. Computations of eigenvalues λ for the phase function $f(x) = \alpha x^3$ using 170×170 matrices.

(this is simply (3.3) with $\alpha = 0$) and

$$B_{mn} = (-i\alpha)^p/p! \qquad (m = n + pq, p = 0, 1, 2, \ldots). \tag{8.9}$$

These two matrices were multiplied together numerically and eigenvalues obtained. The cases $q = 1$ and $q = 2$ (not shown) confirm earlier results and the above discussion. Results for $q = 3$ are given in figure 7. We observe that the picture does differ from the linear shear (back in figure 2(a)) and there is perfect dynamo action for $\alpha \gtrsim 4$. Note that there is still a neutral mode with $|\lambda| = 1$, suggesting that this may be a feature for general phase shifts f.

8.3 Spatial discretisations

In this section we revisit briefly the spatial discretisations mentioned in section 3.4, for which growth rates are shown in figure 3. Recall that the interval $[-1, 1]$ is divided into M equal subintervals, and a power series representation with N terms is used in each. This approach can be justified as we did in sections 6 and 7 above and convergence may be shown as $N \to \infty$ for fixed M. We just sketch the details here.

We have an adjoint eigenfunction given by $\tilde{c} = \{c_j\}$. We demand that each $c_j \in \mathcal{B}$ so that $\tilde{c}$ lies in a Banach space $\tilde{\mathcal{B}} = \mathcal{B}^M$ with norm $\|\tilde{c}\| = \max_j \|c_j\|$. The operator $\tilde{T}^*$ again becomes $\tilde{S}$ and is a bounded, compact operator on $\tilde{\mathcal{B}}$. Again it is possible to project each c_j to a polynomial of N terms to obtain an approximate operator $\tilde{S}_N$ and the eigenvalues will converge as N is increased.

However it is important to note that this piecewise discretisation $\tilde{c} = \{c_j(x)\}$, when reconstructed to give $c(x)$ (cf. (3.9,3.10)) allows eigenfunctions $c(x)$ with discontinuities, which are not in $\mathcal{B}$, but are in L^2. From section 4.2 such discontinuities can only occur at periodic orbits of the underlying tent map, and so depend on the spatial grid, that is the value of M chosen.

To illustrate this figure 8 shows leading adjoint eigenfunctions reconstructed for $\alpha = 2.5$, $M = 48$ and $N = 2$. In figure 8(a,b,d) we recover smooth

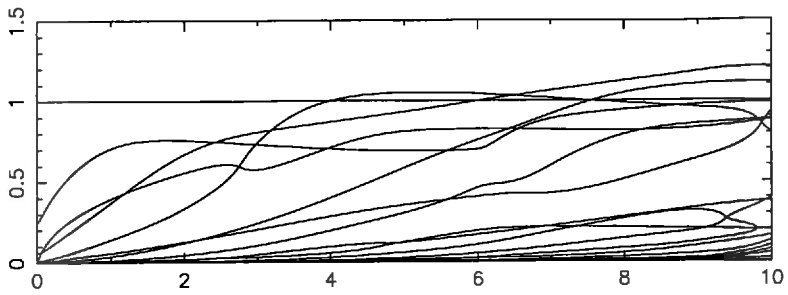

Fig. 7. Computations of eigenvalues λ for the phase function $f(x) = \alpha x^3$ using 170×170 matrices.

(this is simply (3.3) with $\alpha = 0$) and

$$B_{mn} = (-i\alpha)^p/p! \qquad (m = n + pq, p = 0, 1, 2, \ldots). \tag{8.9}$$

These two matrices were multiplied together numerically and eigenvalues obtained. The cases $q = 1$ and $q = 2$ (not shown) confirm earlier results and the above discussion. Results for $q = 3$ are given in figure 7. We observe that the picture does differ from the linear shear (back in figure 2(a)) and there is perfect dynamo action for $\alpha \gtrsim 4$. Note that there is still a neutral mode with $|\lambda| = 1$, suggesting that this may be a feature for general phase shifts f.

8.3 Spatial discretisations

In this section we revisit briefly the spatial discretisations mentioned in section 3.4, for which growth rates are shown in figure 3. Recall that the interval $[-1, 1]$ is divided into M equal subintervals, and a power series representation with N terms is used in each. This approach can be justified as we did in sections 6 and 7 above and convergence may be shown as $N \to \infty$ for fixed M. We just sketch the details here.

We have an adjoint eigenfunction given by $\tilde{c} = \{c_j\}$. We demand that each $c_j \in \mathcal{B}$ so that $\tilde{c}$ lies in a Banach space $\tilde{\mathcal{B}} = \mathcal{B}^M$ with norm $\|\tilde{c}\| = \max_j \|c_j\|$. The operator $\tilde{T}^*$ again becomes $\tilde{S}$ and is a bounded, compact operator on $\tilde{\mathcal{B}}$. Again it is possible to project each c_j to a polynomial of N terms to obtain an approximate operator $\tilde{S}_N$ and the eigenvalues will converge as N is increased.

However it is important to note that this piecewise discretisation $\tilde{c} = \{c_j(x)\}$, when reconstructed to give $c(x)$ (cf. (3.9,3.10)) allows eigenfunctions $c(x)$ with discontinuities, which are not in $\mathcal{B}$, but are in L^2. From section 4.2 such discontinuities can only occur at periodic orbits of the underlying tent map, and so depend on the spatial grid, that is the value of M chosen.

To illustrate this figure 8 shows leading adjoint eigenfunctions reconstructed for $\alpha = 2.5$, $M = 48$ and $N = 2$. In figure 8(a,b,d) we recover smooth

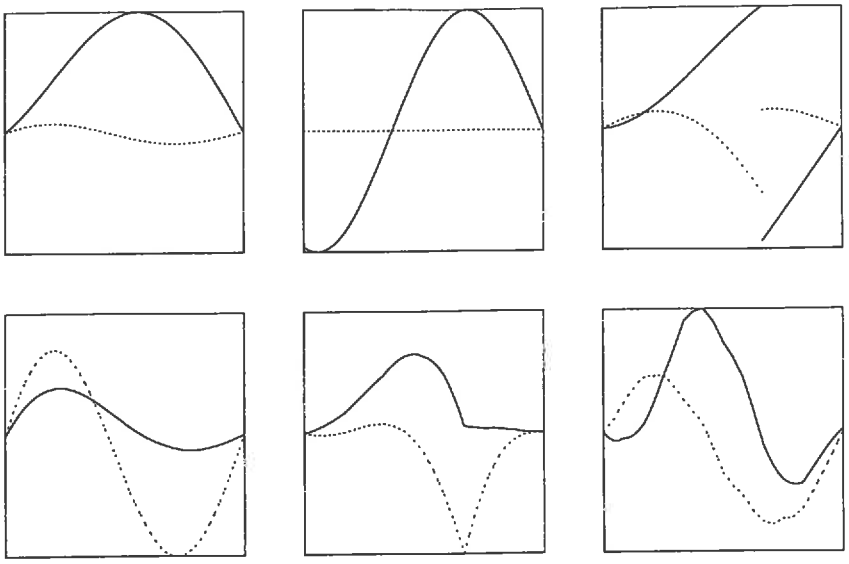

Fig. 8. Adjoint eigenfunctions based on a piecewise linear spatial discretisation plotted as in figure 3, with $M = 48$, $N = 2$ and $\alpha = 2.5$. The top row is (a,b,c) and bottom (d,e,f).

eigenfunctions. However 8(c) shows an eigenfunction with a discontinuity at the fixed point $\frac{1}{3}$ and $|\lambda| = 1$, and in 8(e) there is a discontinuity in derivative there. Finally 8(f) is becoming noisy, as are subsequent eigenfunctions, and these are spurious at this truncation (cf. figure 3(b)). Note that growth rates in figure 3 appear to show convergence as $M \to \infty$ for $N \geq 2$ but not for $N = 1$. It is natural to consider convergence in this limit of refining a spatial grid and it appears that the error is $O(M^{-2})$ for $N = 2$, but we do not have any mathematical justification for this behaviour.

8.4 Flux discretisations

Finally we give a further way of discretising the SFS dynamo. Like taking the adjoint, it turns the contraction of magnetic field structure under the direct operator T into expansion and smoothing of structure. However it retains some properties of the direct operator and may be useful for other models.

Consider a magnetic field $b(x)$ and define

$$\phi(s) = \int_{-1}^{1} e^{-i\alpha s x} b(x)\, dx. \tag{8.10}$$

We call this the *flux function* of the field. Note that $\phi(0)$ is the total flux in the field and $\phi(s)$ is the flux in the field after shearing through αs.

Now if $b(x)$ is mapped under the direct SFS operator T (2.7), then $\phi(s)$ is

mapped under U with

$$U\phi(s) = e^{i\alpha(s+1)/2}\phi(\tfrac{1}{2}(s+1)) - e^{-i\alpha(s+1)/2}\phi(-\tfrac{1}{2}(s+1)). \tag{8.11}$$

This holds without any approximation. U tends to stretch out structure in ϕ. If we only wish to know about the subsequent evolution of the total flux $\phi(0)$ under iteration of U, it is sufficient to know $\phi(s)$ for $s \in [-1,1]$ to determine $U^n\phi(0)$. Perhaps unsurprisingly this operator is equivalent to the adjoint T^* (2.9): if we relate $c(x) = \phi^*(-x)$, then evolution of c under T^* and ϕ under U correspond.

Differences arise when we discretise in space. We can set up a *flux function discretisation*. As in section 3.4 we break $[-1,1]$ into M strips I_j and set

$$\phi_j(s) = \delta \int_{-1}^{1} e^{-i\alpha\delta sx} b_j(x)\, dx, \tag{8.12}$$

so that $\phi(s) = \sum_j e^{-i\alpha\delta s(2j+1)}\phi_j(s)$. This set of functions $\tilde{\phi} = \{\phi_j\}$ again obeys a closed system of equations; under the forward stretch–fold operator T_{SF}, the ϕ_j map according to

$$\tilde{U}_{\mathrm{SF}}\phi_j(s) = \begin{cases} e^{i\alpha\delta s/2}\phi_{M/2+2j}(s/2) + e^{-i\alpha\delta s/2}\phi_{M/2+2j+1}(s/2) & (j<0), \\ -e^{i\alpha\delta s/2}\phi_{M/2-2j-1}(-s/2) - e^{-i\alpha\delta s/2}\phi_{M/2-2j-2}(-s/2) & (j\geq 0), \end{cases} \tag{8.13}$$

and for the shear operator T_{Sh},

$$\tilde{U}_{\mathrm{Sh}}\phi_j(s) = e^{-i\alpha\delta(2j+1)}\phi_j(s+1). \tag{8.14}$$

If we now combine $\tilde{U} = \tilde{U}_{\mathrm{Sh}}\tilde{U}_{\mathrm{SF}}$, we have a prescription for evolving the flux function discretisation, and we only need to know $\phi_j(s)$ for $-1 \leq s \leq 1$. The resulting the resulting operator $\tilde{U}$ looks broadly similar to the adjoint operator $\tilde{T}^*$ in (3.14) above, but closer examination reveals it to be different, because the indices j are mapped differently. In the flux discretisation we have divided the field into strips and in each strip recorded in $\tilde{\phi}$ information about how it responds to shear. When we compute $\tilde{U}\phi_j$ we combine the flux from the two strips which, under the forward SFS map (2.1), are first halved in scale and then mapped into strip I_j. On the other hand the adjoint operator $\tilde{T}^*$ doubles the scale, and then computes $c_j(x)$ from the two expanded strips that overlie I_j. Thus the flux discretisation retains the behaviour of the direct operator $\tilde{T}$, in terms of how the strips are mapped (compare the indices in (8.13) and (3.11)), but within each strip structure as a function of s is stretched out. If we now truncate $\phi_j(s)$ as a power series of N terms, then $N = 1$ corresponds to only recording the fluxes $\phi_j(0)$, $N = 1$ the linear response to shear, and so forth.

In fact the matrices one obtains for the flux discretisation operator $\tilde{U}$ with given N, M are closely related to those for $\tilde{T}^*$ or $\tilde{S}$ (section 3.4) and numerically the eigenvalues found are identical, so figure 3 may be interpreted as results for $\tilde{U}$ as well as for $\tilde{S}$. Thus it appears that to use a flux discretisation, i.e., work with the forward map T, it is necessary to use more information than just fluxes $\phi(0)$ (which would give the incorrect results for $N = 1$ shown in figure 3(a)). We would need to take $N \geq 2$, to obtain results as in figure 3(b) to obtain good results for large M.

We have discussed this discretisation since it offers new approaches to approximating fast dynamos. In particular if one has a hyperbolic two-dimensional model (e.g., [4,17]) with a contracting and expanding direction, x and y say, taking the adjoint operator offers no immediate advantage [8] as it simply exchanges contraction with expansion. Instead one might break up space using a Markov partition and compute a flux function $\phi_j(s, y)$ for each piece, integrating over only the contracting direction x. The resulting discretisation would then be expanding in s and y, with advantages for analysis or numerical computation. However there remain further obstacles. The above discussion of SFS works only for linear phase functions $f(x) = \alpha x$, and so a general phase function $f(x, y)$ in a two-dimensional model would need to be approximated as piecewise linear.

9 Discussion

In this paper we have considered the SFS map with zero diffusion, and studied the direct operator T and its adjoint T^*. The main result of the paper is that SFS has perfect dynamo action: for large enough shear, $\alpha > \pi/2$, we have obtained smooth growing adjoint eigenfunctions. The key to our study is moving from L^2, magnetic fields of finite energy, to a smaller space of analytic magnetic fields, $\mathcal{B}$. In L^2 the operators T and T^* are not compact, and in particular T^* has uncountably many eigenfunctions; however these are not generally smooth. Reducing to the space $\mathcal{B}$ builds in smoothness at the outset, makes the relevant operators compact and allows us to make progress.

Our study has involved a combination of analytical and numerical techniques to establish growth rates with error bounds, based on manipulating finite matrices. A solely analytical approach, for example to show that perfect dynamo action is inevitable for sufficiently large α, remains a challenging problem. One proxmising approach is to use Newton–Raphson iteration and the contraction mapping theorem (Dr. Ben Mestel, personal communication). We also note that perfect dynamo action, as defined in section 1.1, only requires us to obtain smooth eigenfunctions of T or T^*, whereas we have imposed a stronger condition of analyticity. This leaves open an obvious question: are

there smooth eigenfunctions of T or T^* that are not analytic?

In terms of future work, there are several different directions to go from here. The most important is to introduce diffusion and study how perfect dynamo action relates to fast dynamo action: that is the subject of paper II. Here we only mention that, once diffusion is introduced, the dynamo operator in L^2 becomes compact, and so has a discrete family of eigenfunctions and eigenvalues. It is then natural to develop a perturbation theory, which takes the smooth eigenfunctions in this paper and computes modified diffusive growth rates.

Another problem is to extend the above analysis from one dimension to two-dimensional problems, for example cat or pseudo-Anosov maps with shear [4,17]. In this case the direct operator T contracts magnetic field in one direction and expands it in another. Taking the adjoint exchanges these two directions and so offers no obvious simplification (unlike in SFS when a single contracting direction is exchanged for a single expanding one). Possible approaches include using the pinning coordinates of Rugh [29], or the flux discretisation discussed in section 8.4 above, to convert just one contracting direction into an expanding direction. Also the work of Rugh should allow justification of the zeta function methods used to obtain dynamo growth rates [3–5,29].

Finally we reiterate that the key to our analysis was to obtain the correct setting: going from a non-compact operator T^* in L^2 with many unpleasant eigenfunctions, to an operator S on a subset $\mathcal{B} \subset L^2$ for which smoothness is guaranteed. It is the hyperbolicity of the underlying baker's map that is crucial in obtaining compactness (and this is what underlies the study [29]). For a more realistic, smooth fluid flow, for example pulsed Beltrami waves [7,8], this hyperbolicity is lost as the stretching becomes non-uniform at the folds of the map [31,32]. It is far from clear how to restrict the domain of a general dynamo operator T or T^* in a similar way to obtain a compact operator. However this seems the most promising approach for proving results about perfect and fast dynamos in general classes of realistic flows, and so accounting for the apparent robustness of fast dynamo action as observed numerically in wide classes of flows.

A Appendix: the stretch–stack–shear map

In this appendix we define a model similar to SFS, but in which we replace the stretch–fold (SF) operation by a stretch–stack (SSt) operation. This model is much simplified compared with SFS, and allows more explicit calculations [4,12]. It has been used to model the stretch–twist–fold dynamo [14]. The

'stretch–stack' (SSt) operation acts on magnetic fields by

$$T_{\mathrm{SSt}}b(x) = \begin{cases} 2b(1+2x) & (x<0), \\ 2b(-1+2x) & (x>0). \end{cases} \tag{A.1}$$

The adjoint operator is given by

$$T^*_{\mathrm{SSt}}c(x) = c(\tfrac{1}{2}(x-1)) + c(\tfrac{1}{2}(x+1)). \tag{A.2}$$

We may then define a stretch–stack–shear (SStS) operator $T = T_{\mathrm{Sh}}T_{\mathrm{SSt}}$ with adjoint $T^* = T^*_{\mathrm{SSt}}T^*_{\mathrm{Sh}}$. For $\alpha = 0$ the operators T and T^* amplify constant magnetic field, $b = 1$, $\lambda = 2$, and so the SStS model is trivially a perfect dynamo.

The adjoint operator T^* has an infinite family of eigenfunctions

$$c_j(x) = P_j(x)e^{i\alpha x} \quad \lambda_j = 2^{1-j}\cos\alpha \tag{A.3}$$

where $P_j(x)$ is a polynomial of degree j. Thus as α varies, we may trace out smooth branches of eigenvalues. For the direct operator T we know of an explicit eigenfunction only for particular values of α, namely

$$b(x) = e^{i\alpha x}, \quad \lambda = 2e^{i\alpha}, \quad \alpha = n\pi. \tag{A.4}$$

In view of the way in which T reduces scale we suspect that these are the only values of α which allow eigenfunctions of T in L^2. For $\alpha = 0$ it is straightforward to show that T has only the eigenfunction $c = 1$ with $\lambda = 2$, by expanding any eigenfunction in L^2 as a sum of Fourier modes $e^{in\pi x}$.

B Appendix: Eigenfunctions of T for general phase functions

For SFS the direct operator T has no eigenfunctions in L^2 for $\alpha = 0$, and we have not found any eigenfunctions for $\alpha > 0$: recall that an eigenfunction of T must have $|\lambda| = 2$. However the related stretch–fold–stack map (appendix A) has a smooth eigenfunction (A.4) for certain α values. The same is true of the stretch–fold–slide model [21,22]. However these represent cases when the phase shifts are 'just right', and are likely to be non-generic. To support this view let us return to SFS but with a general phase function $f(x)$ (see (2.11)). We will argue that it is exceptional for such a model to have a *continuous* eigenfunction b (and so formalise a similar argument on page 111 of [12]).

Let us take f to be a continuous function on $[-1,1]$ with the supremum norm, $f \in C^0$. Consider a primitive periodic orbit $\boldsymbol{x} = (x_0, x_1, \ldots, x_{m-1})$ of the

tent map (2.6). Suppose T has a continuous eigenfunction b with eigenvalue λ, $|\lambda| = 2$. Evaluating $T^m b = \lambda^m b$ at x_0 yields

$$2^{-m}\lambda^m = \prod_{j=0}^{m-1} \operatorname{sign}(x_j) \exp(-if(x_j)) \equiv \Phi_f(\boldsymbol{x}). \tag{B.1}$$

Provided b does not vanish on this orbit, this gives possible values for the phase ϕ of $\lambda = 2e^{i\phi}$. However taking a different primitive periodic orbit $\boldsymbol{y}$, of period n will generally give an incompatible set of phases. Let $F(\boldsymbol{x}, \boldsymbol{y})$ represent the set of phase functions f for which the phases on the two orbits agree

$$F(\boldsymbol{x}, \boldsymbol{y}) = \{f : \Phi_f(\boldsymbol{x}) = e^{im\phi}, \Phi_f(\boldsymbol{y}) = e^{in\phi} \text{ for some } \phi\}. \tag{B.2}$$

For each pair of orbits the set $F(\boldsymbol{x}, \boldsymbol{y})$ represents a closed subset of C^0 that is nowhere dense, having empty interior. For any f in $C^0 \setminus F(\boldsymbol{x}, \boldsymbol{y})$ the eigenfunction b must vanish either on $\boldsymbol{x}$ or on $\boldsymbol{y}$. By Baire's category theorem (e.g., chapter 5 of [9])

$$C^0 \setminus \bigcup_{\boldsymbol{x},\boldsymbol{y}\,(\boldsymbol{x}\neq\boldsymbol{y})} F(\boldsymbol{x}, \boldsymbol{y}) \tag{B.3}$$

is dense in C^0 (and is of the second category). For any function f in the set (B.3) above, no continuous eigenfunction can exist, as it would be required to vanish on a dense set of orbits.

Thus 'near' to any phase function f there is a phase function for which no continuous eigenfunctions exist, and in this sense, for 'generic' phase functions f no continuous eigenfunctions are possible. However our argument says nothing about general eigenfunctions in L^2, and any results here would be most interesting.

Acknowledgements

I am grateful to Peter Ashwin, Erik Aurell, Bruce Bayly, Steve Childress, Isaac Klapper and Ben Mestel for valuable discussions and references. Erik Aurell first explained the work of H.H. Rugh to me, and Ben Mestel produced a first version of figure 2(a).

Much of this study was carried out at the 'Geometry and Topology of Fluid Flows' programme held at the Isaac Newton Institute in Cambridge (Autumn 2000), and I welcome this opportunity to thank the organisers and director for inviting me to participate in a most interesting programme.

Larger computations were undertaken on the IBM supercomputer 'ceres' at the University of Exeter, supported by the HEFCE JREI.

References

[1] Artuso, R., Aurell, E. & Cvitanović, P. 1990a Recycling of strange sets: I. Cycle expansions. *Nonlinearity* **3**, 325–359.

[2] Artuso, R., Aurell, E. & Cvitanović, P. 1990b Recycling of strange sets: II. Applications. *Nonlinearity* **3**, 361–386.

[3] Aurell, E. 1992 On proving fast dynamo action using (singular) integral operators. Unpublished note.

[4] Aurell, E. & Gilbert, A.D. 1993 Fast dynamos and determinants of singular integral operators. *Geophys. Astrophys. Fluid Dyn.* **73**, 5–32.

[5] Balmforth, N.J., Cvitanović, P., Ierley, G.R., Spiegel, E.A. & Vattay, G. 1993 Advection of vector fields by chaotic flows. In: *Stochastic Processes in Astrophysics*, pp. 148–160. Annals New York Acad. Sci., vol. 706.

[6] Bayly, B.J. 1992 Infinitely conducting dynamos and other horrible eigenproblems. In: *Nonlinear Phenomena in Atmospheric and Oceanic Sciences* (ed. G.F. Carnevale, R.T. Pierrehumbert), pp. 139–176, IMA Series in Mathematics and its Applications, vol. 40. Springer–Verlag.

[7] Bayly, B.J. & Childress, S. 1988 Construction of fast dynamos using unsteady flows and maps in three dimensions. *Geophys. Astrophys. Fluid Dyn.* **44**, 211–240.

[8] Bayly, B.J. & Childress, S. 1989 Unsteady dynamo effects at large magnetic Reynolds numbers. *Geophys. Astrophys. Fluid Dyn.* **49**, 23–43.

[9] Bollobás, B. 1990 *Linear Analysis: An Introductory Course.* Cambridge University Press.

[10] Childress, S. 1992 Fast dynamo theory. In: *Topological Aspects of the Dynamics of Fluids and Plasmas.* (ed. H.K. Moffatt, G.M. Zaslavsky, P. Comte, M. Tabor), pp. 111–147. Kluwer.

[11] Childress, S. 1993 Note on perfect fast dynamo action in a large-amplitude SFS map. In: *Solar and Planetary Dynamos* (ed. M.R.E. Proctor, P.C. Matthews, A.M. Rucklidge), pp. 43–50. Cambridge University Press.

[12] Childress, S. & Gilbert, A.D. 1995 *Stretch, Twist, Fold: The Fast Dynamo.* Springer–Verlag.

[13] Cowling, T.G. 1934 The magnetic field of sunspots. *Mon. Not. Roy. Astr. Soc.* **140**, 39–48.

[14] Finn, J.M. & Ott, E. 1988 Chaotic flows and fast magnetic dynamos. *Phys. Fluids* **31**, 2992–3011.

[15] Finn, J.M., Hanson, J.D., Kan, I. & Ott, E. 1991 Steady fast dynamo flows. *Phys. Fluids B* **3**, 1250–1269.

[16] Galloway, D.J. & Proctor, M.R.E. 1992 Numerical calculations of fast dynamos for smooth velocity fields with realistic diffusion. *Nature* **356**, 691–693.

[17] Gilbert, A.D. 1993 Towards a realistic fast dynamo: models based on cat maps and pseudo-Anosov maps. *Proc. R. Soc. Lond. A* **443**, 585–606.

[18] Gilbert, A.D. 2001 Advected fields in maps: II. Fast dynamo action in the stretch–fold–shear map. In preparation.

[19] Gilbert, A.D. 2001 Advected fields in maps: III. Decay of passive scalars in baker's and related maps. In preparation.

[20] Kato, T. 1980 *Perturbation Theory for Linear Operators.* Springer–Verlag.

[21] Klapper, I. 1991 *Chaotic Fast Dynamos.* PhD Thesis, Courant Institute of Mathematical Sciences, New York University.

[22] Klapper, I. 1992 Kinematic fast dynamo action in a time-periodic chaotic flow. In *Topological Aspects of the Dynamics of Fluids and Plasmas* (ed. H.K. Moffatt, G.M. Zaslavsky, P. Comte, M. Tabor), pp. 563–571. Kluwer Academic Publishers.

[23] Klapper, I. & Young, L.S. 1995 Bounds on the fast dynamo growth rate involving topological entropy. *Comm. Math. Phys.* **173**, 623–646.

[24] de la Llave, R. 1993 Hyperbolic dynamical systems and generation of magnetic fields by perfectly conducting fluids. *Geophys. Astrophys. Fluid Dyn.* **73**, 123–131.

[25] Mather, J.N. 1968 Characterization of Anosov diffeomorphisms. *Indagat. Math.* **30**, 479–483.

[26] Mestel, B.D., Osbaldestin, A.H. & Winn, B. 2000 Golden mean renormalization for the Harper equation: the strong coupling fixed point. *J. Math. Phys.* **41**, 8304–8330.

[27] Moffatt, H.K. 1978 *Magnetic Field Generation in Electrically Conducting Fluids.* Cambridge University Press.

[28] Rado, A. 1993 *Onset and Intermittency in the SFS Map.* MS Thesis, Courant Institute of Mathematical Sciences, New York University.

[29] Rugh, H.H. 1992 The correlation spectrum for hyperbolic analytic maps. *Nonlinearity* **5**, 1237–1263.

[30] Otani, N.F. 1993 A fast kinematic dynamo in two-dimensional time-dependent flows. *J. Fluid Mech.* **253**, 327–340.

[31] Soward, A.M. 1993 An asymptotic solution of a fast dynamo in a two-dimensional pulsed flow. *Geophys. Astrophys. Fluid Dyn.* **73**, 179–215.

[32] Soward, A.M. 1994 On the role of stagnation points and periodic particle paths in a two-dimensional pulsed flow fast dynamo model. *Physica D* **76**, 181–201.

[33] Strang, G. 1989 Wavelets and dilation equations: a brief introduction. *SIAM Review* **31**, 614–627.

[34] Trefethen, L.M. 1997 Pseudospectra of linear operators. *SIAM Review* **39**, 383–406.

[35] Vishik, M.M. 1989 Magnetic field generation by the motion of a highly conducting fluid. *Geophys. Astrophys. Fluid Dyn.* **48**, 151–167.

[36] Zeldovich, Ya.B. 1957 The magnetic field in the two-dimensional motion of a conducting turbulent liquid. *Sov. Phys. JETP* **4**, 460–462.

[37] Zeldovich, Ya.B., Ruzmaikin, A.A. & Sokoloff, D.D. 1983 *Magnetic Fields in Astrophysics.* The Fluid Mechanics of Astrophysics and Geophysics, vol. 3. Gordon & Breach Science Publishers.